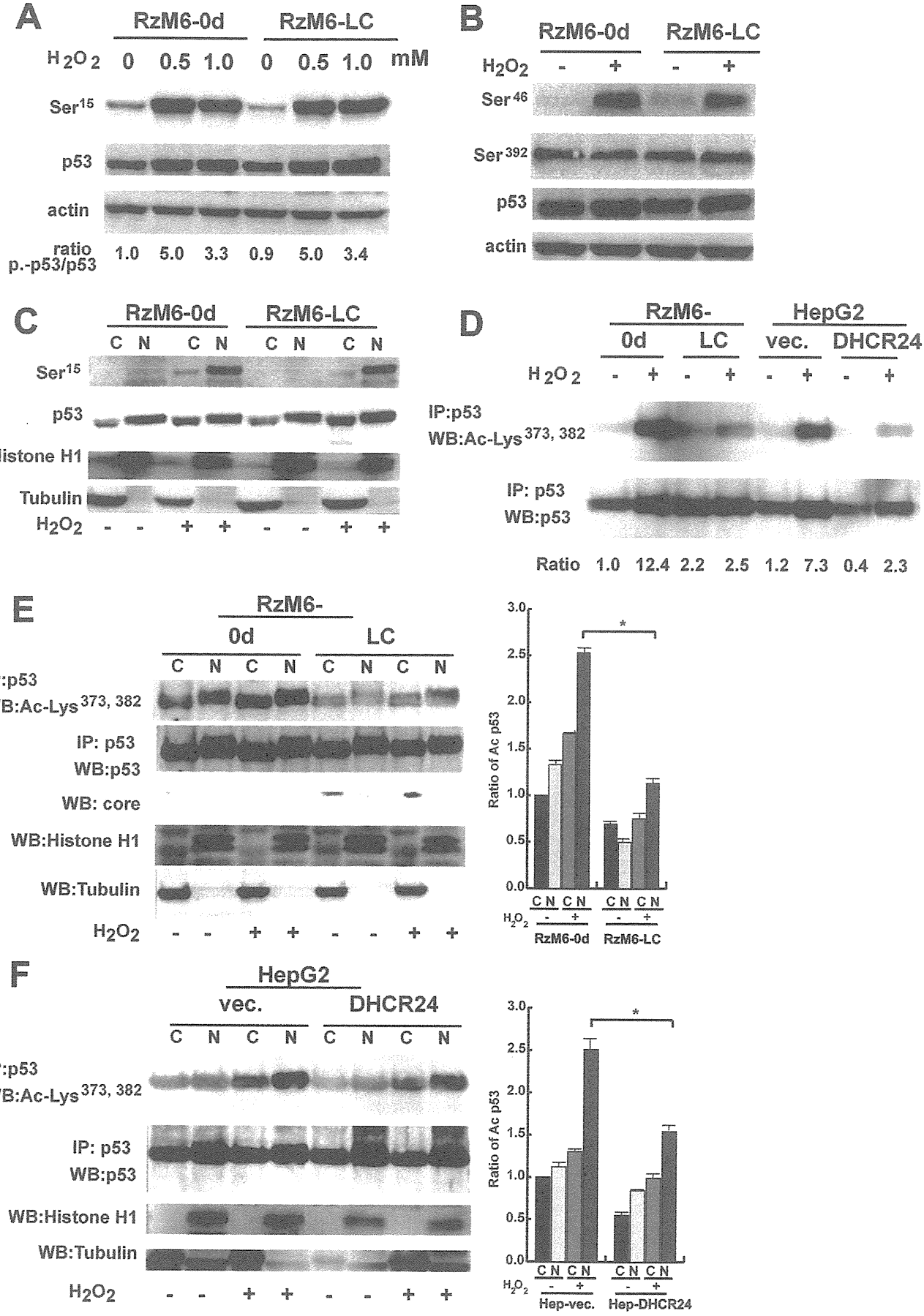

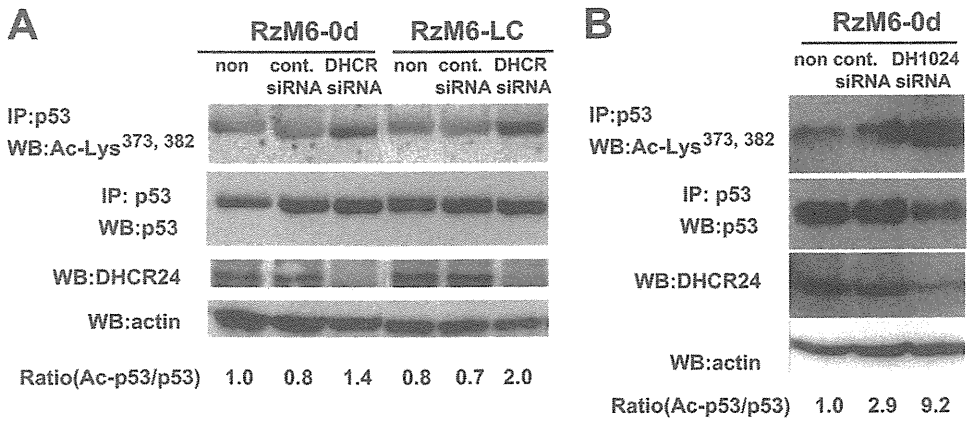

FIGURE 7. **Silencing of DHCR24 increases p53 acetylation.** *A*, RzM6-0d and RzM6-LC cells were untreated (*non*) or treated with control siRNA (*cont. siRNA*) or DHCR24 siRNA. Acetylated p53 Lys^{373} and Lys^{382} (*top*) and total p53 (*bottom*) were immunoprecipitated (*IP*) with anti-p53 antibody (*DO-1*) followed by Western blotting (*WB*), and the expression of actin and DHCR24 by Western blotting (*bottom*) was examined. The average ratio of acetylated p53 to total p53 in RzM6-0d cells without treatment is indicated at the *bottom*. *B*, RzM6-0d cells were transfected with control siRNA (*cont.siRNA*), DHCR24 siRNA (*DH1024* or *DHCR*), or untreated (*non*). Acetylated p53 Lys^{373} and Lys^{382} (*top*) and total p53 (*bottom*) were immunoprecipitated with anti-p53 antibody followed by Western blotting, and the expression of actin and DHCR24 by Western blotting (*bottom*) was examined. Reaction with secondary antibodies (anti-rabbit or mouse IgG conjugated with horseradish peroxidase) alone did not yield any signals (data not shown), and data representative of three independent experiments are shown (*A* and *B*).

treatment (Fig. 5*C*). Silencing of DHCR24 with siRNA decreased the interaction between p53 and MDM2 (supplemental Fig. 2*A*). Overexpression of DHCR24 in HepG2 cells increased the interaction between p53 and MDM2 in the cytoplasm (HepG2-DHCR24; Fig. 5*D* and supplemental Fig. 2, *B* and *C*). Level of p53 in the nucleus after treatment with H_2O_2 was low in RzM6-LC cells (Fig. 5*E*).

In a previous *in vitro* study that used bacterially expressed and purified protein (21), the interaction between p53 and MDM2 was decreased when the amount of DHCR24 was increased. These discrepancies with our results may be due to the different experimental systems. p53 and DHCR24 were induced by H_2O_2 in WI38TERT cells (21), as observed in our system (Fig. 5*F*). However, the interaction between MDM2 and p53 was much lower in WI38 cells than in RzM6 cells (Fig. 5, *G* and *H*). Moreover, ectopic expression of DHCR24 did not inhibit apoptotic response to H_2O_2 in WI38 cells (Fig. 5*I*) but suppressed apoptosis in HepG2 cells (Fig. 3). This different response may be due to the different regulatory systems of p53 and MDM2 in the liver and lung; MDM2 phosphorylation at Ser^{166} is regulated by the MEK-ERK (mitogen-activated protein kinase/extracellular signal-regulated kinase kinase-extracellular signal-regulated kinase) pathway in hepatocytes and Akt in lung cells (29). The response of MDM2 at Ser^{166} to H_2O_2 was significantly high in liver (HepG2) cells but was low in WI38 cells (supplemental Fig. 2, *D* and *E*), as previously observed in A549 cells (29). The up-regulation of MDM2 phosphorylation at Ser^{166} accelerates its E3 ligase activity (30).

We also found that overexpression of DHCR24 did not up-regulate the transcription of *p53* or *MDM2* genes (supplemental Fig. 3, *A* and *B*). However, DHCR24 overexpression inhibited polyubiquitination in RzM6-LC cells and H358 (p53 null) cells (supplemental Fig. 3, *C–E*). This inhibition of polyubiquitination would inhibit p53 degradation, resulting in an increased amount of p53 available to interact with MDM2.

Posttranslational Modification of p53 in DHCR24-overexpressing Cells—We did not detect any *p53* nucleotide substitutions in RzM6-LC cells compared with the *p53* in RzM6-0d cells (data not shown). Thus, we examined the posttranslational modification of p53, which is thought to be tightly connected to the regulation of its function and localization (31). We examined the phosphorylation of p53 at Ser^{15} (Fig. 6*A*); at Ser^{6}, Ser^{9}, Ser^{20}, and Ser^{37} (supplemental Fig. 4*A*); and at Ser^{46} and Ser^{392} (Fig. 6*B*) by Western blotting and found no marked differences in phosphorylation after H_2O_2 treatment between RzM6-0d and RzM6-LC cells. Ser^{15}-phosphorylated p53 was detected in the nuclear fraction of RzM6-0d and RzM6-LC cells after H_2O_2 treatment (Fig. 6*C*). We assessed the acetylation of p53 at Lys^{373} and Lys^{382} by immunoprecipitation followed by Western blotting and found that acetylation of p53 was significantly low in RzM6-LC cells compared with RzM6-0d cells following H_2O_2 treatment (Fig. 6*D*). H_2O_2 induced the acetylation of p53 at Lys^{373} and Lys^{382} in RzM6-0d cells (Fig. 6*E*). This acetylation

FIGURE 6. **Posttranslational modification of p53 in cells overexpressing DHCR24.** *A*, phosphorylation of p53 at Ser^{15} in RzM6-0d and RzM6-LC cells after treatment with 0, 0.5, or 1.0 mM H_2O_2 was examined by Western blotting with specific rabbit polyclonal antibodies. p53 was detected with anti-p53 monoclonal antibody (*DO-1*). Actin was analyzed as a control. *B*, phosphorylation of p53 at Ser^{46} and Ser^{392} in RzM6-0d and RzM6-LC cells after treatment with 0 or 1.0 mM H_2O_2 was analyzed by Western blotting with specific rabbit polyclonal antibodies. p53 was detected with anti-p53 monoclonal antibody. Actin was analyzed as a control. *C*, RzM6-0d or RzM6-LC cells with or without H_2O_2 treatment were fractionated into cytoplasmic (*C*) and nuclear (*N*) fractions that were subjected to Western blotting with the antibodies indicated on the *left*. *D*, acetylation of p53 Lys^{373} and Lys^{382} (*top*) and total p53 (*bottom*) was characterized by immunoprecipitation (*IP*) with anti-p53 antibody followed by Western blotting (*WB*) with the rabbit polyclonal antibodies indicated on the *left* in RzM6-0d and RzM6-LC cells or HepG2 cells transfected with pcDNA vector (*vec.*) or pcDNA-DHCR24 expression vector (*DHCR24*). The average ratio of acetylated p53 to total p53 in RzM6-0d cells without H_2O_2 treatment is indicated at the *bottom*. *E*, acetylation of p53 Lys^{373} and Lys^{382} (*top*) and total p53 (*second panel*) was characterized by immunoprecipitation with anti-p53 antibody followed by Western blotting with the rabbit polyclonal antibodies indicated on the *left* in RzM6-0d and RzM6-LC cells. HCV core protein was detected by Western blotting with monoclonal antibody (31, 32). Cell fractionation was confirmed with antibodies against histone H1 and tubulin. p53 and acetylated p53 were quantitated, and the average ratio of acetylated p53 to total p53 in the cytoplasmic (*C*) fraction of RzM6-0d cells is indicated. *Vertical bars*, S.D. *, $p < 0.05$ (two-tailed Student's *t* test). *F*, acetylation of p53 Lys^{373} and Lys^{382} (*top*) and total p53 (*second panel*) was characterized by IP with anti-p53 antibody followed by Western blotting with the rabbit polyclonal antibodies indicated on the *left* in HepG2 cells transfected with pcDNA vector or pcDNA-DHCR24 vector with or without H_2O_2 treatment. Cell fractionation was confirmed with antibodies against histone H1 and tubulin. p53 and acetylated p53 were quantitated, and the average ratio of acetylated p53 to total p53 in the cytoplasmic fraction of Hep-vec cells is indicated. *Vertical bars*, S.D. *, $p < 0.05$ (two-tailed Student's *t* test). Reaction with secondary antibodies (anti-rabbit or mouse IgG conjugated with horseradish peroxidase) alone did not show any signals (data not shown), and data representative of three independent experiments are indicated (*A–F*).

was significantly inhibited in RzM6-LC cells (Fig. 6*E*). Persistent ectopic overexpression of DHCR24 also repressed H_2O_2-induced p53 acetylation in the nuclei of HepG2 cells (Fig. 6*F*). In addition, silencing of DHCR24 by siRNA caused up-regulation of p53 acetylation at Lys^{373} and Lys^{382} in RzM6-0d and RzM6-LC cells (Fig. 7*A*). When the alternative siRNA for DHCR24 (DH1024) was transfected into RzM6-0d cells, the acetylation of p53 was accelerated (Fig. 7*B*). The mutant DHCR24 vector suppressed the effect of DHCR24 siRNA (supplemental Fig. 4*B*). These results indicate that overexpression of DHCR24 down-regulates p53 acetylation.

DISCUSSION

This study demonstrates that DHCR24 expression parallels hepatocarcinogenesis and that HCV induces overexpression of DHCR24 at both the mRNA and protein levels. Moreover, persistent DHCR24 overexpression suppresses the p53 response to H_2O_2. These findings are consistent with the previous report that inactivation and mutation of p53 plays a role in the development of HCC (32). Hepatocytes with p53 abnormalities are likely to escape from cell cycle check points and acquire resistance to apoptosis, thereby increasing their tumorigenic potential. Likewise, genetic inactivation of p53 is associated with late stage disease (32). HCV RNA levels are notably lower in cancerous tissues from HCV-positive HCC patients than in non-cancerous tissues (33). Thus, impairment of p53 function by HCV-induced DHCR24 overexpression might play a crucial role in early stage disease progression.

In DHCR24-overexpressing cells, p53 was mostly distributed in the cytoplasm (supplemental Fig. 2, *A* and *B*). This change in the distribution pattern of p53 might be caused by an increased interaction between p53 and MDM2, which might be induced by increased phosphorylation of MDM2 and suppression of polyubiquitination by overexpression of DHCR24. The up-regulation of the p53-MDM2 interaction negatively regulates p53 and shuttles p53 from the nucleus to the cytoplasm (34, 35). MDM2 inhibits both *p53* transcriptional activation and p300-mediated p53 acetylation upon ternary complex formation with p300 and p53 (36–38). Acetylation of p53 by CBP/p300 mostly occurs in the nucleus (36). Therefore, the increase in cytoplasmic p53-MDM2 complexes in DHCR24-overexpressing cells may account for the observed suppression of p53 acetylation in the nucleus, even after treatment with H_2O_2 (supplemental Fig. 5). Impaired acetylation of C-terminal lysine residues decreases the sequence-specific DNA-binding activity (39) and the stability of p53 (37, 40). Taken together, our data suggest that DHCR24 overexpression may down-regulate p53 function by inhibiting degradation, increasing the formation of the p53-MDM2 complex in the cytoplasm, and suppressing acetylation of p53 in the nucleus.

In conclusion, we propose that HCV infection impairs the function of p53 through DHCR24 overexpression, which up-regulates the interaction between p53 and MDM2 in the cytoplasm and suppresses p53 acetylation in the nucleus. Because overexpression of DHCR24 is observed in other cancers, including melanoma (24) and prostate cancer (41), the findings from this study might provide a foundation for investigations into the mechanisms underlying the formation of these cancers. We plan to examine the liver-specific regulatory network of the p53-MDM2 interaction by DHCR24 in a future study.

Acknowledgments—We thank S. Imajoh-Ohmi, H. Fukuda, T. Watanabe, S. Nakagawa, K. Tanaka, and R. Takehara for technical support and N. Sonenberg, Y. Furuichi, T. Tsukiyama, S. Tone, S. Sekiguchi, and F. Yasui for valuable comments. We thank S. Harada (Kumamoto University) for kind encouragement.

REFERENCES

1. Choo, Q. L., Kuo, G., Weiner, A. J., Overby, L. R., Bradley, D. W., and Houghton, M. (1989) *Science* **244,** 359–362
2. Tsukiyama-Kohara, K., Iizuka, N., Kohara, M., and Nomoto, A. (1992) *J. Virol.* **66,** 1476–1483
3. Grakoui, A., Wychowski, C., Lin, C., Feinstone, S. M., and Rice, C. M. (1993) *J. Virol.* **67,** 1385–1395
4. Pekow, J. R., Bhan, A. K., Zheng, H., and Chung, R. T. (2007) *Cancer* **109,** 2490–2496
5. Lauer, G. M., and Walker, B. D. (2001) *N. Engl. J. Med.* **345,** 41–52
6. Saito, I., Miyamura, T., Ohbayashi, A., Harada, H., Katayama, T., Kikuchi, S., Watanabe, Y., Koi, S., Onji, M., Ohta, Y., *et al.* (1990) *Proc. Natl. Acad. Sci. U.S.A.* **87,** 6547–6549
7. Shepard, C. W., Finelli, L., and Alter, M. J. (2005) *Lancet Infect. Dis.* **5,** 558–567
8. Kiyosawa, K., Umemura, T., Ichijo, T., Matsumoto, A., Yoshizawa, K., Gad, A., and Tanaka, E. (2004) *Gastroenterology* **127,** S17–S26
9. Parkin, D. M. (2001) *Lancet Oncol.* **2,** 533–543
10. Hussain, S. P., Schwank, J., Staib, F., Wang, X. W., and Harris, C. C. (2007) *Oncogene* **26,** 2166–2176
11. Tardif, K. D., Waris, G., and Siddiqui, A. (2005) *Trends Microbiol.* **13,** 159–163
12. Levrero, M. (2006) *Oncogene* **25,** 3834–3847
13. Tsukiyama-Kohara, K., Toné, S., Maruyama, I., Inoue, K., Katsume, A., Nuriya, H., Ohmori, H., Ohkawa, J., Taira, K., Hoshikawa, Y., Shibasaki, F., Reth, M., Minatogawa, Y., and Kohara, M. (2004) *J. Biol. Chem.* **279,** 14531–14541
14. Köhler, G., and Milstein, C. (1975) *Nature* **256,** 495–497
15. Yasui, K., Wakita, T., Tsukiyama-Kohara, K., Funahashi, S. I., Ichikawa, M., Kajita, T., Moradpour, D., Wands, J. R., and Kohara, M. (1998) *J. Virol.* **72,** 6048–6055
16. Tsukiyama-Kohara, K., Poulin, F., Kohara, M., DeMaria, C. T., Cheng, A., Wu, Z., Gingras, A. C., Katsume, A., Elchebly, M., Spiegelman, B. M., Harper, M. E., Tremblay, M. L., and Sonenberg, N. (2001) *Nat. Med.* **7,** 1128–1132
17. Watanabe, T., Sudoh, M., Miyagishi, M., Akashi, H., Arai, M., Inoue, K., Taira, K., Yoshiba, M., and Kohara, M. (2006) *Gene. Ther.* **13,** 883–892
18. Iivonen, S., Hiltunen, M., Alafuzoff, I., Mannermaa, A., Kerokoski, P., Puoliväli, J., Salminen, A., Helisalmi, S., and Soininen, H. (2002) *Neuroscience* **113,** 301–310
19. Greeve, I., Hermans-Borgmeyer, I., Brellinger, C., Kasper, D., Gomez-Isla, T., Behl, C., Levkau, B., and Nitsch, R. M. (2000) *J. Neurosci.* **20,** 7345–7352
20. Waterham, H. R., Koster, J., Romeijn, G. J., Hennekam, R. C., Vreken, P., Andersson, H. C., FitzPatrick, D. R., Kelley, R. I., and Wanders, R. J. (2001) *Am. J. Hum. Genet.* **69,** 685–694
21. Wu, C., Miloslavskaya, I., Demontis, S., Maestro, R., and Galaktionov, K. (2004) *Nature* **432,** 640–645
22. Wakita, T., Pietschmann, T., Kato, T., Date, T., Miyamoto, M., Zhao, Z., Murthy, K., Habermann, A., Kräusslich, H. G., Mizokami, M., Bartenschlager, R., and Liang, T. J. (2005) *Nat. Med.* **11,** 791–796
23. Kuehnle, K., Crameri, A., Kälin, R. E., Luciani, P., Benvenuti, S., Peri, A., Ratti, F., Rodolfo, M., Kulic, L., Heppner, F. L., Nitsch, R. M., and Mohajeri, M. H. (2008) *Mol. Cell. Biol.* **28,** 539–550
24. Di Stasi, D., Vallacchi, V., Campi, V., Ranzani, T., Daniotti, M., Chiodini, E., Fiorentini, S., Greeve, I., Prinetti, A., Rivoltini, L., Pierotti, M. A., and Rodolfo, M. (2005) *Int. J. Cancer* **115,** 224–230
25. Lois, C., Hong, E. J., Pease, S., Brown, E. J., and Baltimore, D. (2002) *Science*

295, 868–872
26. Yamamoto, H., Ozaki, T., Nakanishi, M., Kikuchi, H., Yoshida, K., Horie, H., Kuwano, H., and Nakagawara, A. (2007) *Genes Cells* **12,** 461–471
27. Miyashita, T., and Reed, J. C. (1995) *Cell* **80,** 293–299
28. Yu, J., Zhang, L., Hwang, P. M., Kinzler, K. W., and Vogelstein, B. (2001) *Mol. Cell* **7,** 673–682
29. Malmlöf, M., Roudier, E., Högberg, J., and Stenius, U. (2007) *J. Biol. Chem.* **282,** 2288–2296
30. Gottlieb, T. M., Leal, J. F., Seger, R., Taya, Y., and Oren, M. (2002) *Oncogene* **21,** 1299–1303
31. Bode, A. M., and Dong, Z. (2004) *Nat. Rev. Cancer* **4,** 793–805
32. Farazi, P. A., and DePinho, R. A. (2006) *Nat. Rev. Cancer* **6,** 674–687
33. Tanaka, T., Inoue, K., Hayashi, Y., Abe, A., Tsukiyama-Kohara, K., Nuriya, H., Aoki, Y., Kawaguchi, R., Kubota, K., Yoshiba, M., Koike, M., Tanaka, S., and Kohara, M. (2004) *J. Med. Virol.* **72,** 223–229
34. Roth, J., Dobbelstein, M., Freedman, D. A., Shenk, T., and Levine, A. J. (1998) *EMBO J.* **17,** 554–564
35. Freedman, D. A., and Levine, A. J. (1998) *Mol. Cell. Biol.* **18,** 7288–7293
36. Kobet, E., Zeng, X., Zhu, Y., Keller, D., and Lu, H. (2000) *Proc. Natl. Acad. Sci. U.S.A.* **97,** 12547–12552
37. Ito, A., Lai, C. H., Zhao, X., Saito, S., Hamilton, M. H., Appella, E., and Yao, T. P. (2001) *EMBO J.* **20,** 1331–1340
38. Ohkubo, S., Tanaka, T., Taya, Y., Kitazato, K., and Prives, C. (2006) *J. Biol. Chem.* **281,** 16943–16950
39. Gu, W., and Roeder, R. G. (1997) *Cell* **90,** 595–606
40. Yuan, Z. M., Huang, Y., Ishiko, T., Nakada, S., Utsugisawa, T., Shioya, H., Utsugisawa, Y., Yokoyama, K., Weichselbaum, R., Shi, Y., and Kufe, D. (1999) *J. Biol. Chem.* **274,** 1883–1886
41. Bonaccorsi, L., Luciani, P., Nesi, G., Mannucci, E., Deledda, C., Dichiara, F., Paglierani, M., Rosati, F., Masieri, L., Serni, S., Carini, M., Proietti-Pannunzi, L., Monti, S., Forti, G., Danza, G., Serio, M., and Peri, A. (2008) *Lab. Invest.* **88,** 1049–1056

GASTROENTEROLOGY 2009;137:285–296

BASIC—LIVER, PANCREAS, AND BILIARY TRACT

Hepatitis C Virus and Disrupted Interferon Signaling Promote Lymphoproliferation via Type II CD95 and Interleukins

KEIGO MACHIDA,[*,‡,§] KYOKO TSUKIYAMA-KOHARA,[*,‖] SATOSHI SEKIGUCH,[*] EIJI SEIKE,[¶] SHIGENOBU TÓNE,[#] YUKIKO HAYASHI,[**] YOSHIMI TOBITA,[*] YURI KASAMA,[‖] MASUMI SHIMIZU,[‡‡] HIDEMI TAKAHASHI,[‡‡] CHYOJI TAYA,[§§] HIROMICHI YONEKAWA,[§§] NOBUYUKI TANAKA,[‡,‖‖] and MICHINORI KOHARA[*]

[*]Department of Microbiology and Cell Biology, Tokyo Metropolitan Institute of Medical Science, Tokyo, Japan; [‡]Department of Immunology, Graduate School of Medicine and Faculty of Medicine, University of Tokyo, Tokyo, Japan; [§]Department of Molecular Microbiology and Immunology, Keck School of Medicine, University of Southern California, Los Angeles, California; [‖]Department of Experimental Phylaxiology, Faculty of Medical and Pharmaceutical Sciences, Kumamoto University, Kumamoto, Japan; [¶]Department of Internal Medicine, Self-Defense Forces Central Hospital, Tokyo, Japan; [#]Department of Biochemistry, Kawasaki Medical School, Okayama, Japan; [**]Department of Pathology, Tokyo Metropolitan Komagome Hospital, Tokyo, Japan; [‡‡]Department of Microbiology and Immunology, Nippon Medical School, Tokyo, Japan; [§§]Laboratory of Animal Science, Tokyo Metropolitan Institute of Medical Science, Tokyo, Japan; and [‖‖]Department of Molecular Oncology, Institute of Gerontology, Nippon Medical School, Kanagawa, Japan

BACKGROUND & AIMS: The molecular mechanisms of lymphoproliferation associated with the disruption of interferon (IFN) signaling and chronic hepatitis C virus (HCV) infection are poorly understood. Lymphomas are extrahepatic manifestations of HCV infection; we sought to clarify the molecular mechanisms of these processes. **METHODS:** We established interferon regulatory factor-1–null (irf-$1^{-/-}$) mice with inducible and persistent expression of HCV structural proteins (irf-1/CN2 mice). All the mice (n = 900) were observed for at least 600 days after Cre/loxP switching. Histologic analyses, as well as analyses of lymphoproliferation, sensitivity to Fas-induced apoptosis, colony formation, and cytokine production, were performed. Proteins associated with these processes were also assessed. **RESULTS:** *Irf-1*/CN2 mice had extremely high incidences of lymphomas and lymphoproliferative disorders and displayed increased mortality. Disruption of *irf-1* reduced the sensitivity to Fas-induced apoptosis and decreased the levels of caspases-3/7 and caspase-9 messenger RNA species and enzymatic activities. Furthermore, the *irf-1*/CN2 mice showed decreased activation of caspases-3/7 and caspase-9 and increased levels of interleukin (IL)-2, IL-10, and Bcl-2, as well as increased Bcl-2 expression, which promoted oncogenic transformation of lymphocytes. IL-2 and IL-10 were induced by the HCV core protein in splenocytes. **CONCLUSIONS: Disruption of IFN signaling resulted in development of lymphoma, indicating that differential signaling occurs in lymphocytes compared with liver. This mouse model, in which HCV expression and disruption of IFN signaling synergize to promote lymphoproliferation, will be an important tool for the development of therapeutic agents that target the lymphoproliferative pathway.**

More than 175 million people worldwide are infected with hepatitis C virus (HCV), which is a positive-strand RNA virus that infects both hepatocytes and peripheral blood mononuclear cells.[1–4] Chronic hepatitis infection can lead to hepatitis, cirrhosis, hepatocellular carcinoma, and lymphoproliferative diseases, such as B-cell non-Hodgkin's lymphomas and mixed cryoglobulinemia.[5–10] The current therapy for chronic HCV infection involves treatment with type I interferon (IFN) and derivatives of IFN, such as pegylated IFN.[11] Treatment with type I IFN is associated with regression of lymphoma in patients with hepatitis C.[12] However, more than 50% of HCV-infected individuals are resistant to treatment, which indicates that the inhibition of IFN signal transduction facilitates the persistent expression of HCV proteins by hepatocytes.

Transgenic mice that express the HCV core protein have been established using a promoter derived from hepatitis B virus,[13] whereas mice that express structural or complete viral proteins have been established using promoters derived from the albumin gene.[14] These mice are immunotolerant to the transgene and do not develop hepatic inflammation, although they do develop age-related hepatic steatosis and hepatocellular carcinomas. We also developed a transgenic mouse model in which the HCV complementary DNA, including viral genes that encode the core, E1, E2, and NS2 proteins, was conditionally expressed by the Cre/*lox*P system (CN2 mice).[15]

Abbreviations used in this paper: IFN, interferon; IL, interleukin; IRF, interferon-regulatory factor; PCR, polymerase chain reaction; WT, wild-type.

0016-5085/09/$36.00
doi:10.1053/j.gastro.2009.03.061

The conditional expression of HCV proteins protected mice from Fas-mediated lethal acute liver failure by inhibiting cytochrome *c* release from the mitochondria.[16] However, the expression of HCV in these mice was usually lost after 21 days. Therefore, an animal model of persistent HCV protein expression is required to examine the effects of chronic HCV infection in vivo.

IFN signaling mediates tumor suppressor effects and antiviral responses and is regulated by key transcription factors of the interferon-regulatory factor (IRF) protein family, including Irf-1, -2, -3, -7, and -9. Targeted disruption of *irf-1* results in aberrant lymphocyte development and a marked reduction in the number of $CD8^+$ T cells in the peripheral blood, spleen, and lymph nodes.[17] In addition, natural killer cell development is impaired in *irf-1*$^{-/-}$ mice.[18] The mechanisms by which HCV infection induces IFN resistance and influences the development of lymphomas are poorly understood. Therefore, in the present study, we established an *irf-1*$^{-/-}$ CN2 mouse model of persistent HCV expression, which allows investigation of the effects of HCV on lymphatic tissue tumor development.

Materials and Methods

Animal Experiments

Wild-type (WT), CN2, *irf-1*$^{-/-}$, and *Mx1-cre* mice were maintained in conventional animal housing under specific pathogen-free conditions. AxCANCre and AxCAw1 were obtained from Dr Izumu Saito (University of Tokyo).[15] To elicit Fas-induced liver damage, adult mice were injected intravenously with 10 μg of purified hamster monoclonal antibody against mouse Fas (clone Jo2; BD Biosciences, San Diego, CA) in 200 μL of phosphate-buffered saline. All animal experiments were performed according to the guidelines of the Tokyo Metropolitan Institute of Medical Science or Kumamoto University Subcommittee for Laboratory Animal Care. The protocol was approved by an institutional review board. Detailed procedures, including induction of the HCV transgene by poly(I:C) in CN2-29 Mx1-Cre mice, are described in Supplementary Materials and Methods.

Measurements of Caspase Activities

The cytosolic splenocyte fractions were isolated as described,[16] and the detailed procedures are described in the Supplementary Material and Methods.

Lentiviral Vectors and Infection

Isolated splenocytes from WT or *irf-1*$^{-/-}$ mice (total of 10^7 cells) were infected with recombinant lentiviruses that express HCV core, E1, E2, NS2, *lacZ*, and empty vector, respectively. One day after infection, cells were selected with puromycin (final concentration of 1 μg/mL). After 5 days of puromycin selection, viable cells were examined.

Baculovirus Expression and Purification of HCV Core, E1, and E2 Proteins

The E1 and E2 sequences from a genotype 1a isolate (strain H77)[19] and a genotype 1b isolate (strain HC-J4),[20] without the C-terminal transmembrane domains but containing the His_6 tag at the C terminus, were cloned into a transfer vector (pBlueBacHis2; Invitrogen, Carlsbad, CA). The expression of recombinant core, E1, and E2 proteins in insect cells and their purification have been described previously.[21]

Results

Viral Protein Expression and Disruption of irf-1 Synergistically Increase the Development of Lymphoproliferative Disorders

To clarify the in vivo effects of HCV protein expression, we examined the survival of mice that carry the CN2 transgene (CN2-8, CN2-29).[15] The experimental design is shown in Figure 1*A* (total number of mice, 900). Without Cre/*lox*P switching, the animals that carry the HCV transgene (CN2-8 and CN2-29: core, E1, E2, and NS2 proteins) appeared healthy and developed normally.[15] All of the transgene carriers were observed for at least 600 days after Cre/*lox*P switching (Figure 1*A*). Administration of a recombinant adenovirus that expresses *cre* (AxCANCre) induced the efficient recombination of CN2 transgenes in the hepatocytes from CN2 and *irf-1*$^{-/-}$ CN2 mice (Figure 1*B*). Recombination produced the floxed CN2 transgene (3.3 kilobases) and was completed within 4–7 days; it diminished before day 21 in CN2 mice but persisted in *irf-1*$^{-/-}$ CN2 mice. The expression of core protein in the hepatocytes of CN2 mice peaked on day 7 and decreased to an undetectable level by day 21 (Supplementary Figure 1*A*). The expression of core protein in hepatocytes coincided with a high level of inflammation, as determined by measurements of serum alanine aminotransferase activity (Supplementary Figure 1*A* and data not shown). The HCV core protein was detected in CN2-8 mice 4–14 days after the administration of AxCANCre, and disruption of *irf-1* ensured core protein expression for more than 500 days (Supplementary Figure 1*A* and 1*B*). Therefore, *irf-1* disruption allowed efficient and persistent expression of HCV proteins. HCV core protein gene expression was confirmed by reverse-transcription polymerase chain reaction (PCR) of livers, splenocytes, and peripheral blood monocytes (Supplementary Figure 1*C*). AxCANCre administration to the transgenic mouse induced the efficient expression of HCV transgenes in lymphocytes and splenocytes (Supplementary Figure 1*C*).

The survival rate of WT mice injected with the *cre*-adenovirus (AxCANCre) (Figure 1*C*) or control adenovirus (AxCAw1) (data not shown) was higher than that of the transgenic mice (CN2-8 and CN2-29), which excludes the possibility that the recombinant adenovirus affec-

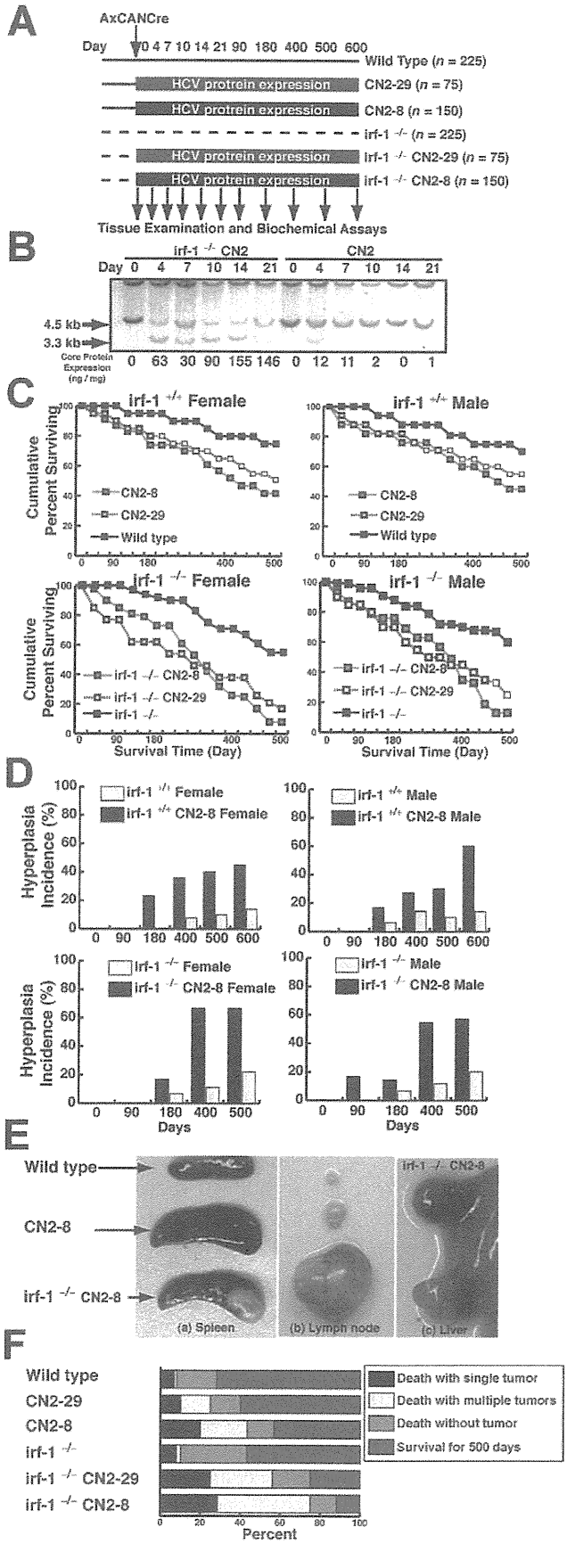

ted the results. More than 75% of the WT mice injected with AxCANCre survived to day 500, whereas the HCV-expressing mice had lower survival rates. The *irf-1*$^{-/-}$ CN2-8 and *irf-1*$^{-/-}$ CN2-29 strains had even lower survival rates, indicating that persistent HCV protein expression in combination with *irf-1* disruption significantly decreases survival (Figure 1*C*).

Lymphoproliferative Disorders Are Accelerated With Age and Level of Viral Protein Expression

To determine the mechanism underlying the increased mortality caused by persistent HCV protein expression in *irf-1*$^{-/-}$ CN2 mice, we examined the kinetics of dysplasia (Figure 1*D*). Strikingly, 67% of the female *irf-1*$^{-/-}$ CN2 mice and 70% of the male *irf-1*$^{-/-}$ CN2 mice developed tumors 400 days after the administration of AxCANCre. Some of the *irf-1*$^{-/-}$ CN2 mice developed hyperplasia of the lymph nodes, and these tumors developed much earlier than the tumors in their *irf-1*$^{+/+}$ or CN2 counterparts (Figure 1*D*). Aberrant cell proliferation developed randomly among the male and female carrier animals between day 180 and day 600. On day 400 after Cre/*lox*P switching, the average weights of the spleens of the WT, CN2, and *irf-1*$^{-/-}$ CN2 mice were 90, 160, and 310 mg, respectively. The disruption of *irf-1* aggravated the HCV-induced spontaneous proliferative disturbances in lymphatic tissues. The number of CN2 mice that died with at least one tumor and the number of tumors per

Figure 1. Disruption of *irf-1* enhances oncogenic potential in combination with HCV transgene expression. (*A*) Experimental design for the animal model. Transgenic mice and their nontransgenic littermates (10–14 weeks of age) were administered the *Cre*-expressing adenovirus (AxCANCre) and killed after 4, 7, 10, 14, 21, 90, 120, 400, 500, or 600 days. (*B*) Southern blot analysis of hepatocyte DNA from mice derived by crossing *irf-1*$^{-/-}$ and HCV-transgenic (CN2) mice. Genomic DNA samples from WT (+/+) and CN2 mouse hepatocytes were digested with *Xba*I and subjected to Southern blot analysis using a radiolabeled genomic flanking probe to determine the rate of recombination of the HCV transgene construct (3.3-kilobase fragment). Disruption of *irf-1* allows persistent expression of HCV proteins. The effects of HCV protein expression on the survival rates of male and female *irf-1*$^{-/-}$ and *irf-1*$^{+/+}$ CN2 mice are shown. (*C*) Kaplan–Meier survival curves for WT mice, *irf-1*$^{-/-}$ mice, CN2 transgenic mouse strains 8 and 29, and *irf-1*$^{-/-}$ CN2-8 and CN-29 mice following infection with a recombinant adenovirus that expresses *cre* (AxCANCre). (*D*) HCV protein expression enhances hyperplasia in male and female CN2 and *irf-1*$^{-/-}$ CN2 mice. The occurrence of hyperplasia was monitored every 7 days for 600 days following the administration of AxCANCre. (*E*) Spleens (*a*) and lymph nodes (*b*) from age-matched WT, CN2, and *irf-1*$^{-/-}$ CN2 mice 500 days after the administration of AxCANCre. (*c*) Liver from the same *irf-1*$^{-/-}$ CN2 mouse (developing severe lymphadenopathy and splenomegaly) following the administration of AxCANCre. (*F*) The cause of death in CN2 transgenic mice with hyperplasias. Mice of each genotype (n = 150) were monitored up to day 600 after the administration of AxCANCre, and necropsies were performed to determine the number of tumors. Tumors included thymomas, splenomas, lymphomas, and hepatocellular carcinomas.

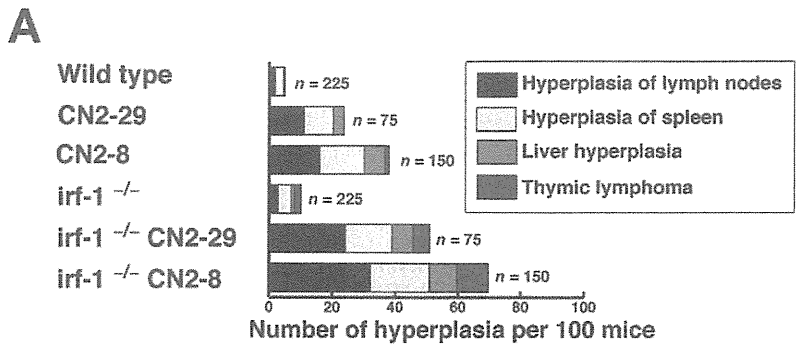

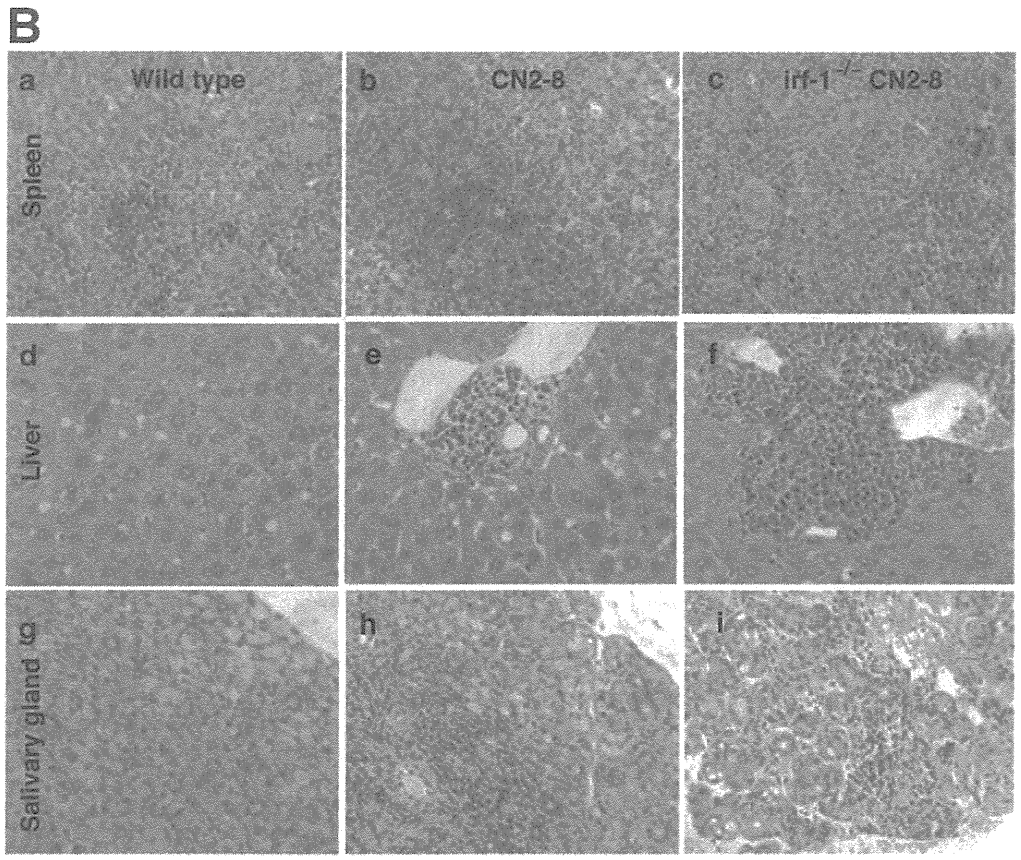

Figure 2. Disruption of *irf-1* aggravates lymphocyte infiltration in combination with HCV transgene expression. (*A*) Histologic analysis of spontaneous proliferative disturbances in the CN2 transgenic mice. Of the 900 mice injected with AxCANCre, 25 of 75 (33%) CN2-29, 47 of 150 (31%) CN2-8, 29 of 75 (39%) *irf-1*$^{-/-}$ CN2-29, and 62 of 150 (41%) *irf-1*$^{-/-}$ CN2-8 mice developed proliferative disturbances. Data shown are from the same cohort of mice analyzed in Figure 1*F*. (*B*) H&E-stained tissue sections of (*a–c*) spleens, (*d–f*) livers, and (*g–i*) salivary glands from age-matched WT, CN2, and *irf-1*$^{-/-}$ CN2 mice after the administration of AxCANCre.

mouse were significantly increased by the ablation of *irf-1* (Figure 1*F*). Although the type of hyperplasia did not differ significantly between the *irf-1*$^{-/-}$ CN2 mice and their *irf-1*$^{+/+}$ CN2 siblings, the time to onset of tumorigenesis differed dramatically (Figure 1*D* and 1*F*), indicating that age is a significant factor in the promotion of lymphomagenesis by HCV proteins.

A significant percentage of the mice that expressed the HCV core protein (*irf-1*$^{-/-}$ CN2 mice) developed polyclonal lymphoid growth disturbances, including splenomegaly, expanded lymph nodes, adenocarcinoma in the abdomen or leg, and lymphoma of the liver or Peyer's patches (Figure 2*A*). In contrast, hepatocytes with abundant expression of HCV proteins rarely developed into hepatocellular carcinomas. H&E staining of splenomegalic tissue revealed extensive hyperplasia of the white pulp zones, in which the cortical zones contained lymphoid follicles and scattered germinal centers, although mitotic figures were rarely observed (Figure 2*B* and data not shown). These results indicate that persistent expression of HCV proteins frequently induces lymphoproliferative disorders in addition to liver hyperplasia, which is consistent with the phenotype of patients with hepatocellular carcinoma.[3,4,9]

Abnormal T-Cell and B-Cell Proliferation in HCV Transgenic Mice

To characterize the disruption of lymphocyte proliferation due to HCV protein expression in the transgenic mice, we used flow cytometry to determine the ratio of T cells to B cells by staining with antibodies directed against CD3, CD45R, CD4, CD8, and the T-cell receptor. The average ratio of T cells to B cells in the lymph nodes and spleens of CN2 mice was significantly higher than

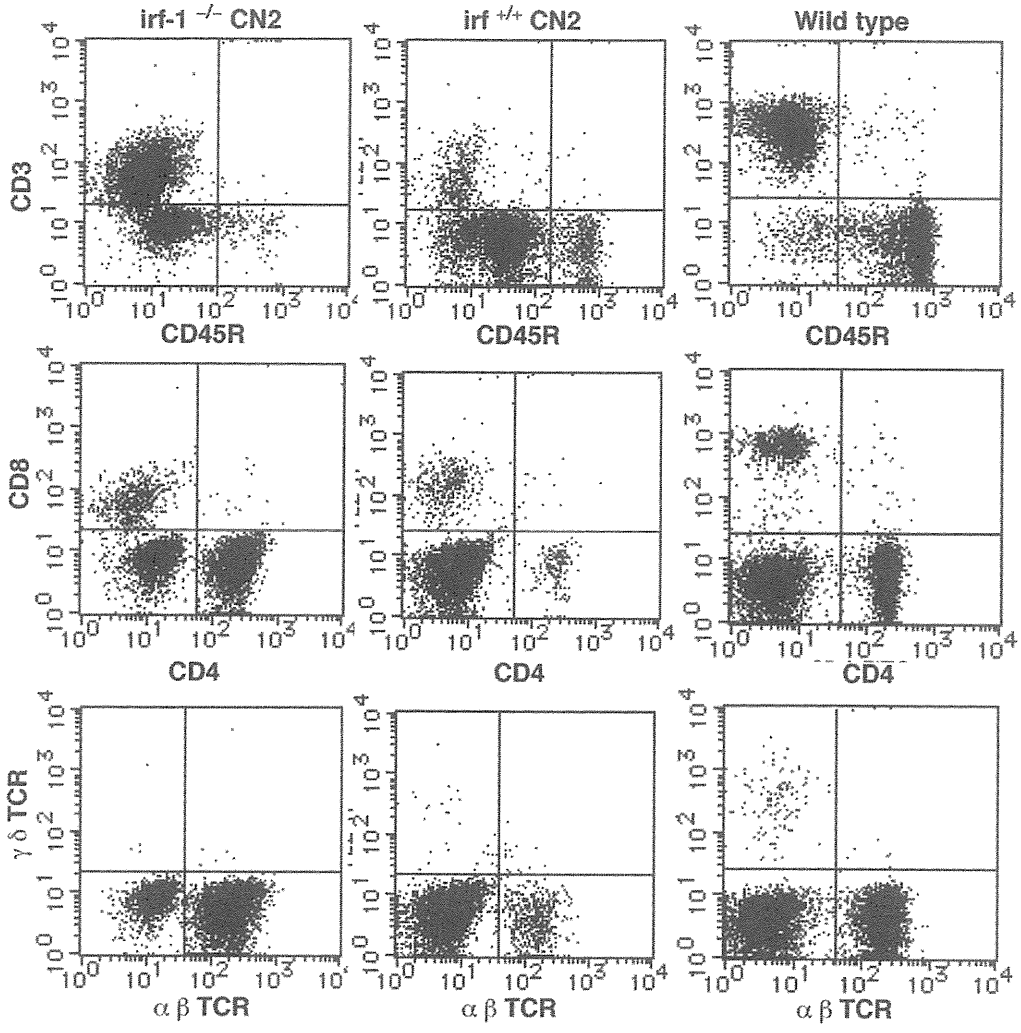

Figure 3. HCV expression and *irf-1* ablation affect the lymphocyte population. T-cell and B-cell proliferation in *irf-1*$^{+/+}$ CN2 mice, *irf-1*$^{-/-}$ CN2 mice, and WT mice. CD3$^+$, CD45R$^+$, CD4$^+$, CD8$^+$, and T-cell receptor–positive cells from age-matched *irf-1*$^{-/-}$ CN2, *irf-1*$^{+/+}$ CN2, and WT mice with hyperplasia were analyzed by fluorescence-activated cell sorting. Lymphocytes were prepared from CN2-8 and WT littermates at the age of 16 months, after administration of AxCANCre for 400 days.

that in the WT mice. The majority of the CD3$^+$ lymphocytes and a few CD8$^+$ lymphocytes expressed CD4 on their surfaces. The proliferating cells were mainly CD4$^+$ T cells, although some were CD45R$^+$B cells (Figure 3 and data not shown). The *irf-1*$^{-/-}$ CN2 mice also developed B-cell lymphomas (data not shown). These results confirm that HCV protein expression induces lymphoproliferative disorders that involve excessive expansion of both T and B cells. In *irf-1*$^{-/-}$ CN2 mice, the cell population that was negative for T-cell receptor (α, β, γ, and δ isoforms) staining was smaller than that in the other mice.

Inhibition of Fas-Induced Apoptosis Owing to Disruption of irf-1 *Leads to Persistent Expression of HCV in Transgenic Mouse Livers*

The Fas ligand is essential for the development of hepatitis via cytotoxic T-lymphocyte–mediated cell killing.[22] Therefore, we determined the sensitivities of *irf-1*$^{-/-}$ hepatocytes to Fas-induced apoptosis. The *irf-1*$^{-/-}$ mice and WT littermates were injected intravenously with a monoclonal antibody against Fas. The disruption of *irf-1* inhibited Fas-induced apoptosis, presumably by decreasing the levels of caspase-6 and -7 messenger RNA (mRNA; Supplementary Figure 2). These results suggest that the reduced expression of effector caspases delays Fas-mediated apoptosis in *irf-1*$^{-/-}$ mice and abrogates the elimination of HCV-expressing cells in vivo.

Stable Expression of HCV Proteins Induces Lymphoproliferative Diseases

To confirm that HCV proteins induce lymphoproliferation without the adenoviral vector system, switching of the expression of HCV proteins was conducted using the Mx promoter–driven cre recombinase with poly(I:C) induction (Figure 4*A*). The Mx promoter is active in hepatocytes as well as in hematopoietic cells. We crossed CN2 mice with Mx1-Cre transgenic mice; CRE recombinase was expressed from the IFN-inducible *Mx1* promoter. Injection of the Mx1-Cre/CN2-29 mice with poly (I:C) induced IFN production and efficiently induced the generation of CN2 gene products in hematopoietic cells

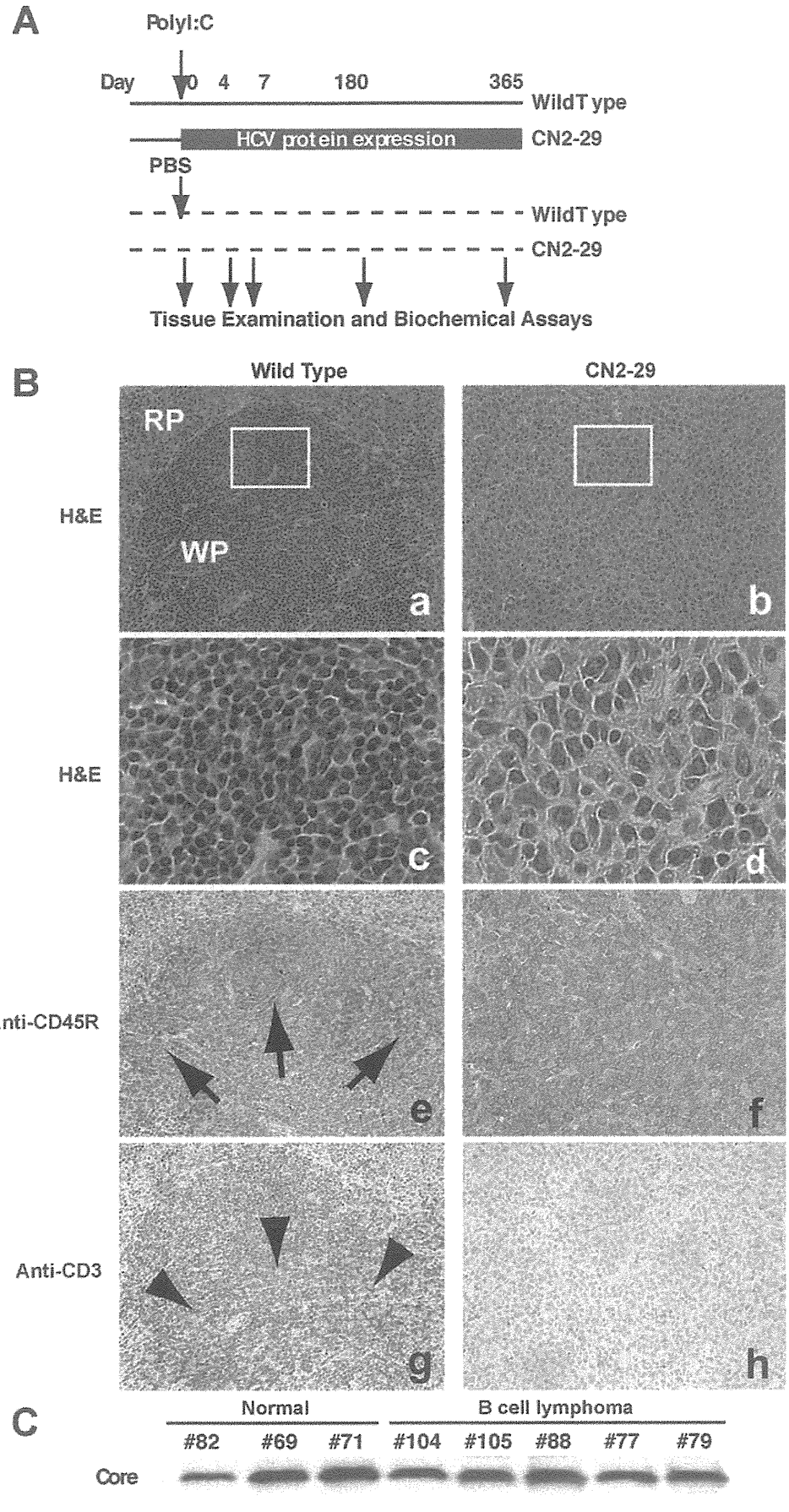

Figure 4. Stable expression of HCV viral proteins induces lymphoproliferative diseases. (*A*) Switching of the expression of HCV proteins was conducted using the Mx promoter–driven cre recombinase with poly(I:C) induction. The Mx promoter is active in hepatocytes as well as in hematopoietic cells. We crossed CN2 mice with Mx1-Cre transgenic mice; Cre recombinase was expressed from the IFN-inducible *Mx1* promoter. Injection of Mx1-Cre/CN2-29 mice with poly(I:C) induces IFN production and efficiently induces the expression of CN2 gene products in hematopoietic cells (mainly in Kupffer cells and lymphocytes), livers, and spleens but not in most other tissues. (*B*) The white pulp (WP) and red pulp (RP) comprise the components of the spleen in WT mice. The neoplastic cells replace the normal structures, such as the white pulp and red pulp. (*c* and *d*) The neoplastic cells are larger than lymphocytes (*c*), and the nuclei are irregular, round, oval, elongated, and polygonal (*d*). (*e* and *g*) The white pulp in WT mice consists of both a B-cell–rich area (*arrows*, *e*) and T-cell–rich area (*arrowheads*, *g*). (*f* and *h*) The neoplastic cells show staining for the B-cell marker CD45R, thereby supporting the diagnosis of B-cell lymphoma (*f*), while they do not show staining for the T-cell marker CD3 (*h*). *Frames c* and *d* are higher-magnification views of the white box areas in *a* and *b*, respectively. (*C*) Core protein expression was confirmed by immunoblotting.

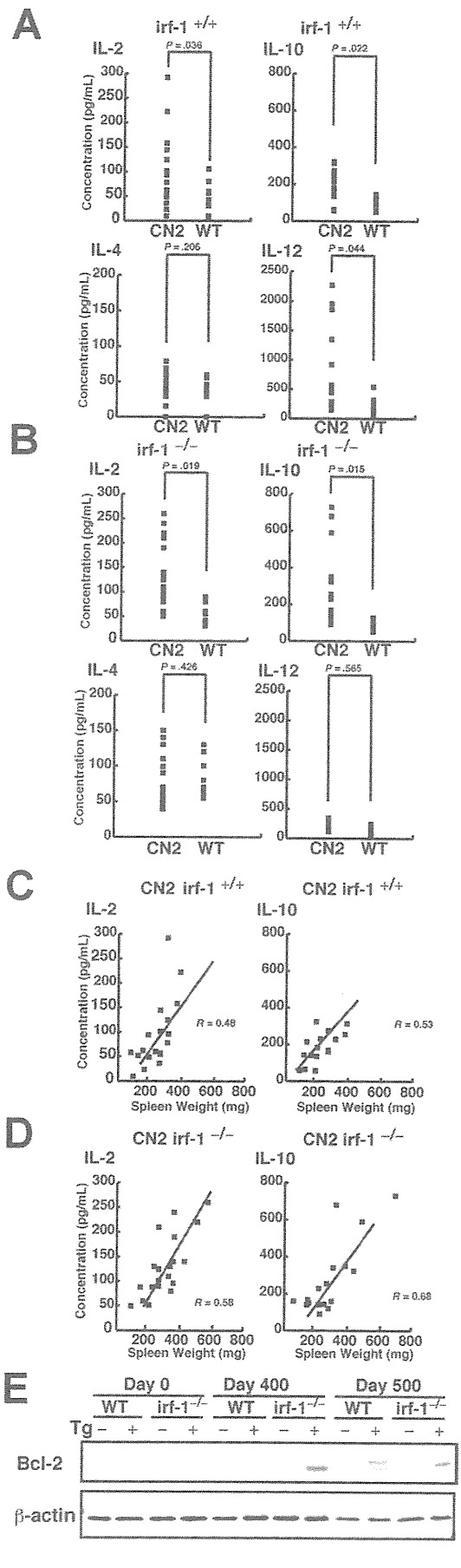

(mainly in Kupffer cells and lymphocytes), liver, and spleen but not in most other tissues. At 7 days after induction of viral proteins, HCV core proteins were detected in both hepatocytes and hematopoietic cells (data not shown). After 180 days, almost 40% of the CN2(-29) mice developed lymphomas, whereas the WT mice did not (Figure 4*B*). The neoplastic cells were larger than lymphocytes, and their nuclei were irregular, round, oval, elongated, and polygonal. HCV core protein expression was confirmed by immunoblotting (Figure 4*C*), and increases in the levels of interleukin (IL)-2, IL-10, and IL-12 were observed (data not shown). The hematopoietic marker CD45R was detected in the lymphoproliferative regions and spleens (Figure 4*B*). The efficiency of expression switching was confirmed by both the HCV transgene copy numbers and protein expression using quantitative PCR and immunoblotting, respectively (Supplementary Figure 3). These results further validate that sustained expression of HCV proteins induces lymphoproliferation.

Increased IL-2, IL-10, and IL-12 Levels in HCV Transgenic Mice

To study the mechanisms of HCV-induced lymphoproliferative diseases, we measured the serum IL-2, IL-4, IL-10, and IL-12 levels in the CN2 transgenic mice and their WT littermates (Figure 5*A*). The serum IL-4 concentration did not differ significantly between the CN2 and WT mice following injection with AxCANCre. However, the CN2 mice had significantly increased levels of serum IL-2, IL-10, and IL-12. Notably, the CN2 mice with proliferative disturbances in the lymph nodes and spleen had dramatically elevated levels of these cytokines, suggesting that altered cytokine production is involved in aberrant lymphocyte proliferation or differentiation in CN2 mice. In contrast, the *irf-1*$^{-/-}$ CN2 mice did not show elevated levels of serum IL-12 but had significantly higher levels of serum IL-2 and IL-10 compared with *irf-1*$^{-/-}$ mice (Figure 5*B*). Thus, the disruption of *irf-1* abrogates the increase in IL-12 level but augments the increases in the levels of IL-2 and IL-10 in CN2 mice. These results indicate that IL-2 and IL-10 play key roles

Figure 5. HCV protein expression alters the cytokine profile. (*A*) The serum IL-2, IL-4, IL-10, and IL-12 levels in *irf-1*$^{+/+}$ CN2 (Tg+) and *irf-1*$^{+/+}$ WT mice were measured by enzyme-linked immunosorbent assay. (*B*) The serum IL-2, IL-4, IL-10, and IL-12 levels in *irf-1*$^{-/-}$ CN2 (Tg+) and *irf-1*$^{-/-}$ WT mice were measured by enzyme-linked immunosorbent assay. The *P* values are based on comparisons of the mean cytokine concentrations. (*C* and *D*) Relationship between the IL-2 or IL-10 concentration in the serum and the spleen weights of (*C*) CN2irf-1$^{+/+}$ or (*D*) CN2irf1$^{-/-}$ mice with progressive lymphoproliferation. The numbers of points in the graphs correspond to the numbers of tested animals. (*E*) Bcl-2 protein levels in the lymph nodes of *irf-1*$^{+/+}$ (WT) and *irf-1*$^{-/-}$ transgenic (CN2) (Tg+) and WT mice on days 0, 400, and 500 after the administration of AxCANCre. Bcl-2 migrates at 26 kilodaltons. β-Actin was used as a loading control.

in the induction of the lymphoproliferative phenotype in *irf-1*$^{-/-}$ CN2 mice.

To verify the relationship between the weights of the lymph organs and the cytokine levels, the correlation coefficients were calculated according to Pearson (Figure 5*C* and 5*D*). Whereas spleen weight did not markedly influence the increase in IL-4 level (data not shown), a significant positive correlation was found between spleen weight and increased IL-2 and IL-10 levels in CN2 gene-expressing mice on the *irf-1*$^{-/-}$ background ($R = 0.58$, $P < .05$, and $R = 0.68$, $P < .05$, respectively) (Figure 5*D*). With respect to the serum levels of IL-2 and IL-10, a less intensive but significant positive correlation was found between the cytokine levels and spleen weights of CN2 gene-expressing mice on the *irf-1*$^{+/+}$ background ($R = 0.43$, $P < .05$, and $R = 0.53$, $P < .05$, respectively) (Figure 5*C*). These results indicate that IL-2 and IL-10 are involved in lymphoproliferation in viral protein-expressing mice.

Aberrant Expression of Bcl-2 in Expanded Lymph Nodes of CN2 Mice

Bcl-2 immunoglobulin transgenic mice develop follicular lymphoproliferation[23] due to the inability of various stimuli to induce apoptosis in these mice.[24] Therefore, to examine whether HCV causes dysregulation of Bcl-2 in lymphoid tissues, we examined the expression of Bcl-2 (Figure 5*E*). Lymph nodes collected from *irf-1*$^{-/-}$ CN2 mice 400 days after the administration of AxCANCre showed elevated levels of Bcl-2. Immunoblot analysis revealed that a doublet for Bcl-2 (26 and 28 kilodaltons) appeared in some samples 500 days after AxCANCre administration, suggesting the presence of phosphorylated and nonphosphorylated Bcl-2.[25]

Combination Cytokine Treatment Enhances Splenocyte Colony Formation in Synergy With Viral Protein Expression

To determine whether aberrant cytokine profiles contribute to lymphocyte transformation, a colony formation assay was performed using the methylcellulose method. Mouse splenocytes were infected with adenoviruses that expressed the *cre* DNA recombinase or *lacZ* control. Expression of HCV core proteins was induced by cre-adenovirus infection of the splenocytes (Figure 6*A*). Colony counting was performed at postinfection day 28 (Figure 6*B*). Combined treatment with IL-2 and IL-10 greatly enhanced colony formation, especially in the splenocytes of HCV transgenic mice (CN2-29, *irf-1*$^{-/-}$ CN2-29). The addition of IL-12 suppressed colony formation induced by combined treatment with IL-2 and IL-10. In the *irf-1*$^{-/-}$ background, treatment with IL-2 plus IL-10 or IL-2 plus IL-12 greatly enhanced colony formation. To determine whether enhanced colony formation correlated with cytokine-induced Bcl-2 expression, the Bcl-2 mRNA levels in the splenocytes were quantified (Figure 6*C*). Because IL-2 enhances T-lymphocyte proliferation and transformation,[26] it is of particular interest that treatment with IL-2 plus IL-10 resulted in marked increases in both lymphocyte transformation and the Bcl-2 mRNA levels upon HCV transgene expression. These results indicate that dysregulated cytokine expression, disruption of *irf-1*, and HCV transgene expression synergistically enhance splenocyte transformation.

Cytokine Treatment and HCV Transgene Expression Synergistically Inhibit Fas-Mediated Apoptosis

To determine whether cytokines inhibit Fas-induced apoptosis, we treated the splenocytes from transgenic and WT mice with cytokines and then measured Fas-induced apoptosis by Annexin V staining and fluorescence-activated cell sorting, and we also assayed caspase enzymatic activity (Figure 6*D* and 6*E*). IL-10 treatment in the presence of IL-2 greatly inhibited Fas-induced apoptosis. Furthermore, *irf-1* disruption made the splenocytes resistant to Fas-induced apoptosis in the presence of IL-2, IL-10, and/or IL-12. In particular, IL-2 plus IL-10 treatment produced the strongest inhibition of Fas-induced apoptosis. These cytokines also up-regulated the Bcl-2 mRNA levels in splenocytes, which indicates that IL-2, IL-10, and/or IL-12 up-regulate *bcl-2* expression, which subsequently inhibits Fas-induced apoptosis. This result is consistent with reports that IL-10 and/or IL-2 treatment induce *bcl-2* in B or T lymphocytes.[10,27] Caspase-3/7 activity was correlated with the level of *bcl-2* expression (Figure 6*C* and 6*F*). These results indicate that aberrant cytokine expression and disruption of IFN signaling affect *bcl-2* expression, which is associated with the inhibition of caspase expression.

HCV Core and E2 Proteins Mediate IL-2, IL-10, and IL-12 Expression

To determine which viral protein is responsible for cytokine expression, individual viral proteins were stably expressed in splenocytes using recombinant lentiviruses that express the HCV core, E1, E2, NS2, and lacZ. Each gene expression profile was confirmed by reverse-transcription PCR (Supplementary Figure 4). Only the HCV core protein induced IL-2 and IL-10 (Figure 7*A*). To determine whether extracellular viral proteins trigger cytokine expression, recombinant viral proteins were added to the cells. Only the viral envelope protein E2 induced IL-12 (Figure 7*B*). These results indicate that the HCV core and E2 proteins are responsible for IL-2, IL-10, and IL-12 expression.

HCV Core and IL-10 Induce Bcl-2 Expression

To determine whether viral protein expression and cytokine stimulation synergistically induce Bcl-2 expression, individual viral proteins were stably expressed using lentiviral vectors, and the cells were tested for Bcl-2 expression. Core protein expression and IL-10 stimula-

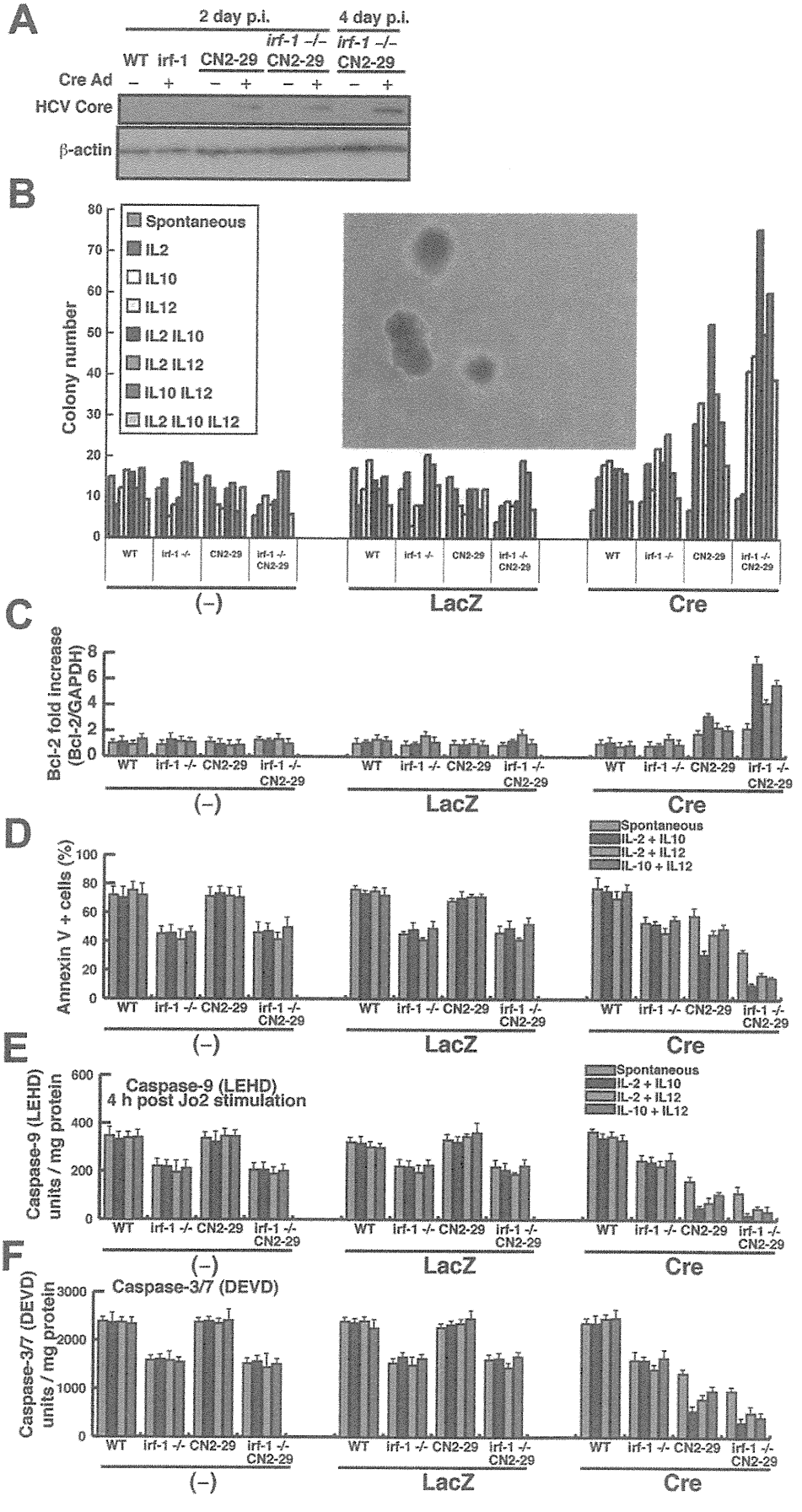

Figure 6. Lymphocyte transformation by aberrant cytokines and inhibition of apoptotic signaling. (*A*) Expression of the HCV core protein (21 kilodaltons) in *irf-1*$^{+/+}$ (WT) and *irf-1*$^{-/-}$ transgenic (CN2-29) and WT mice 2 or 4 days postinfection (p.i.) with AxCANCre (multiplicity of infection, 1.0). β-Actin was used as a loading control. (*B*) Colony formation assay for splenocytes from *irf-1*$^{+/+}$ (WT) and *irf-1*$^{-/-}$ WT or transgenic (CN2-29) mice in the absence or presence of the indicated cytokine and infected with mock, LacZ, and Cre adenoviruses. The *inset* shows an image of the colonies generated from the *irf-1*$^{-/-}$ CN2 splenocytes (original magnification 10×). (*C*) Quantification, by quantitative reverse-transcription PCR of Bcl-2 mRNA relative to control glyceraldehyde-3-phosphate dehydrogenase mRNA in the splenocytes of *irf-1*$^{+/+}$ (WT) and *irf-1*$^{-/-}$ or transgenic (CN2-29) mice treated with the indicated cytokines and infected with mock, LacZ, and cre adenoviruses. (*D*) Apoptosis measured by Annexin V fluorescence-activated cell sorting analysis of splenocytes from *irf-1*$^{+/+}$ (WT) and *irf-1*$^{-/-}$ or transgenic (CN2-29) mice treated with the indicated cytokines and infected with the mock, LacZ, and cre adenoviruses. (*E* and *F*) The caspase-9 and caspase-3/7 enzymatic activities in splenocytes from *irf-1*$^{+/+}$ (WT) and *irf-1*$^{-/-}$ or transgenic (CN2-29) mice treated with the indicated cytokines were measured using a substrate cleavage assay after infection with the mock, LacZ, and Cre adenoviruses. Caspase-9 activity was measured 4 hours after injection of the anti-Fas monoclonal antibody (Jo2). LEHD, substrate for caspase-9; DEVD, substrate for caspase-3/7. Vertical bars are SD and were determined using the Student *t* test.

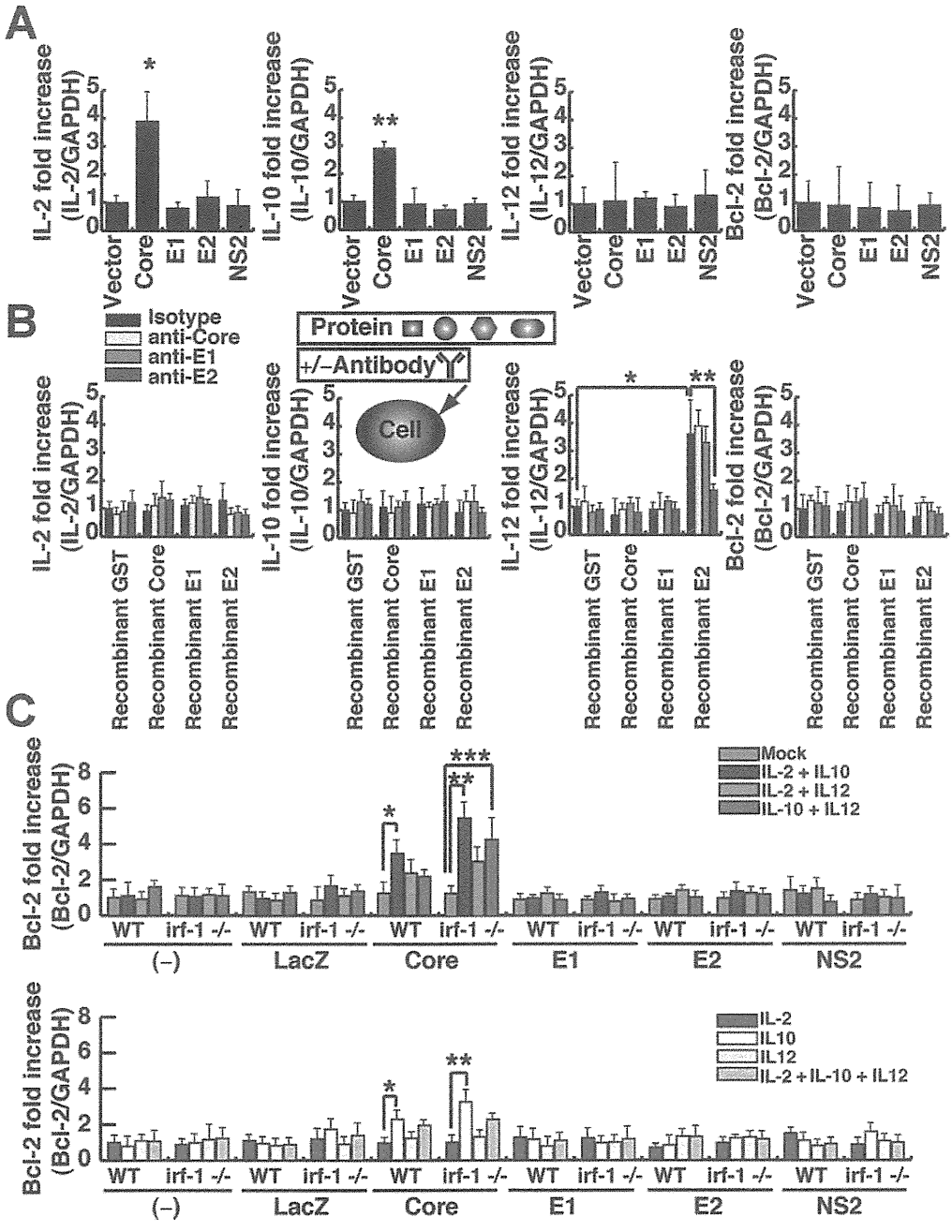

Figure 7. Induction of IL-2 and IL-10 by HCV core and IL-12 by E2 and of Bcl-2 by HCV core plus cytokines. (*A*) Individual viral proteins were stably expressed in splenocytes using recombinant lentiviruses that expressed the HCV core, E1, E2, NS2, and lacZ. Each gene expression profile was determined by quantitative reverse-transcription PCR. (*B*) E2 binding induces IL-12 in Raji cells, as determined by quantitative reverse-transcription PCR. Cells were treated with HCV core, E1, E2 (genotypes 1a and 1b), or glutathione *S*-transferase proteins, and the cytokine and bcl2 cellular RNA levels were examined using quantitative reverse-transcription PCR. (*C*) Quantification by quantitative reverse-transcription PCR of Bcl-2 mRNA relative to control glyceraldehyde-3-phosphate dehydrogenase mRNAin splenocytes from *irf-1*$^{+/+}$ (WT) and *irf-1*$^{-/-}$ WT or irf-1$^{-/-}$ mice treated with the indicated cytokines and infected with lentiviruses that express mock, core, E1, E2, NS2, and LacZ. Individual viral proteins were stably expressed using lentiviral vectors, and the cells were tested for Bcl-2 expression.

tion induced Bcl-2, while the other proteins did not (Figure 7C). Interestingly, the combination of IL-2 and IL-12 only induced Bcl-2 in the *irf-1*$^{-/-}$ background, while triple stimulation (IL-2, IL-10, and IL-12) did not induce Bcl-2 (Figure 7C). These results indicate that complex signaling networks induce Bcl-2 in the presence of viral nucleocapsid proteins.

Discussion

The present study shows that Bcl-2 levels, cytokine levels, aging, and inflammation enhance the development of lymphoproliferative disorders caused by HCV proteins (Supplementary Figure 5). Disruption of *irf-1* enables the persistent expression of HCV protein, leading to lymphoproliferative diseases owing to reduced apoptosis (ie, lower levels of caspase-1, -6, and -7 expression). HCV CN2 transgenic (Tg+) mice are resistant to Fas-induced apoptosis due to the inhibition of cytochrome *c* release from mitochondria.[16] Mice with disruption of *irf-1* have several defects of their innate and adaptive immunity, such as lineage-specific defects in thymocyte development; immature T cells can develop into mature CD4$^+$ cells but not into CD8$^+$ T cells.[18,28] IRF-1 controls the positive and negative selection of CD8$^+$ thymocytes.[29] IRF-1 is required for the development of the Th1-type immune response, and

its absence leads to the induction of the Th2-type immune response.[18,30] Because the number of natural killer cells is dramatically reduced in *irf-1*$^{-/-}$ mice,[18] this defect may cause the marked increase in viral protein expression and the inhibition of tumor surveillance mechanisms, leading to the development of non-Hodgkin's lymphoma. Expression of the IL-12 p40 subunit is defective in *irf-1*$^{-/-}$ mice.[18]

Lymphomagenesis may require the additional genetic instability provided by HCV-induced hypermutation (2-hit model). Important questions are raised regarding the lymphoproliferative mechanisms of lymphomas in HCV-infected patients (B-cell malignancies predominate). Hypermutation of the immunoglobulin genes in B cells induced by HCV infection is the cause of the lymphomagenesis seen in HCV infection,[21,31] and this model may provide more direct insights into lymphoma production, because HCV-induced hypermutation causes genetic instability and causes chromosomal aberrations, possibly resulting in neoplastic transformation.[32] In addition, the antiapoptotic phenotype generated by sustained viral protein expression may enhance the survival of lymphocytes and inhibit activation-induced cell death to turn off the activated lymphocytes. The dysregulated cytokine profiles and sustained lymphocyte survival may alter the fates of regulatory T cells and dendritic cells.[33]

In conclusion, the present study shows that the conditional expression of HCV proteins induces inflammation and lymphoproliferative disorders, which are enhanced by *irf-1* disruption. Therefore, IRF-1–inducible genes probably play essential roles in suppressing HCV-induced lymphoma and in eliminating HCV protein-expressing cells. Our transgenic mice provide evidence that the overexpression of apoptosis-related proteins, including Bcl-2, and/or aberrant cytokine production are primary events in HCV-induced lymphoproliferation. It is interesting to note that lymphoproliferation was dominant over liver tumor development in the present study. Approximately 40% of the CN2-29Mx1Cre mice developed B-cell lymphomas, while 5% of the mice developed liver tumors. Further molecular analyses will enlighten the differential signaling pathways between hepatocytes and lymphocytes and increase our understanding of the differences between lymphomagenesis and liver tumor development caused by HCV.

Supplementary Data

Note: To access the supplementary material accompanying this article, visit the online version of *Gastroenterology* at www.gastrojournal.org, and at doi: 10.1053/j.gastro.2009.03.061.

References

1. Saito I, Miyamura T, Ohbayashi A, et al. Hepatitis C virus infection is associated with the development of hepatocellular carcinoma. Proc Natl Acad Sci U S A 1990;87:6547–6549.
2. Simonetti RG, Camma C, Fiorello F, et al. Hepatitis C virus infection as a risk factor for hepatocellular carcinoma in patients with cirrhosis. A case-control study. Ann Intern Med 1992;116: 97–102.
3. Ferri C, Monti M, La Civita L, et al. Infection of peripheral blood mononuclear cells by hepatitis C virus in mixed cryoglobulinemia. Blood 1993;82:3701–3704.
4. Silvestri F, Pipan C, Barillari G, et al. Prevalence of hepatitis C virus infection in patients with lymphoproliferative disorders. Blood 1996;87:4296–4301.
5. Rui L, Goodnow CC. Lymphoma and the control of B cell growth and differentiation. Curr Mol Med 2006;6:291–308.
6. Dietrich CF, Lee JH, Herrmann G, et al. Enlargement of perihepatic lymph nodes in relation to liver histology and viremia in patients with chronic hepatitis C. Hepatology 1997;26:467–472.
7. Ascoli V, Lo Coco F, Artini M, et al. Extranodal lymphomas associated with hepatitis C virus infection. Am J Clin Pathol 1998; 109:600–609.
8. De Vita S, De Re V, Sansonno D, et al. Gastric mucosa as an additional extrahepatic localization of hepatitis C virus: viral detection in gastric low-grade lymphoma associated with autoimmune disease and in chronic gastritis. Hepatology 2000;31: 182–189.
9. Mele A, Pulsoni A, Bianco E, et al. Hepatitis C virus and B-cell non-Hodgkin lymphomas: an Italian multicenter case-control study. Blood 2003;102:996–999.
10. Cohen SB, Crawley JB, Kahan MC, et al. Interleukin-10 rescues T cells from apoptotic cell death: association with an upregulation of Bcl-2. Immunology 1997;92:1–5.
11. Pawlotsky JM. The nature of interferon-alpha resistance in hepatitis C virus infection. Curr Opin Infect Dis 2003;16:587–592.
12. Levine AM, Shimodaira S, Lai MM. Treatment of HCV-related mantle-cell lymphoma with ribavirin and pegylated interferon alfa. N Engl J Med 2003;349:2078–2079.
13. Moriya K, Fujie H, Shintani Y, et al. The core protein of hepatitis C virus induces hepatocellular carcinoma in transgenic mice. Nat Med 1998;4:1065–1067.
14. Lerat H, Honda M, Beard MR, et al. Steatosis and liver cancer in transgenic mice expressing the structural and nonstructural proteins of hepatitis C virus. Gastroenterology 2002;122:352–365.
15. Wakita T, Taya C, Katsume A, et al. Efficient conditional transgene expression in hepatitis C virus cDNA transgenic mice mediated by the Cre/loxP system. J Biol Chem 1998;273:9001–9006.
16. Machida K, Tsukiyama-Kohara K, Seike E, et al. Inhibition of cytochrome c release in Fas-mediated signaling pathway in transgenic mice induced to express hepatitis C viral proteins. J Biol Chem 2001;276:12140–12146.
17. Yokota T, Oritani K, Takahashi I, et al. Adiponectin, a new member of the family of soluble defense collagens, negatively regulates the growth of myelomonocytic progenitors and the functions of macrophages. Blood 2000;96:1723–1732.
18. Taki S, Sato T, Ogasawara K, et al. Multistage regulation of Th1-type immune responses by the transcription factor IRF-1. Immunity 1997;6:673–679.
19. Yanagi M, Purcell RH, Emerson SU, et al. Transcripts from a single full-length cDNA clone of hepatitis C virus are infectious when directly transfected into the liver of a chimpanzee. Proc Natl Acad Sci U S A 1997;94:8738–8743.
20. Yanagi M, St Claire M, Shapiro M, et al. Transcripts of a chimeric cDNA clone of hepatitis C virus genotype 1b are infectious in vivo. Virology 1998;244:161–172.
21. Machida K, Cheng KT, Pavio N, et al. Hepatitis C virus E2-CD81 interaction induces hypermutation of the immunoglobulin gene in B cells. J Virol 2005;79:8079–8089.

22. Kondo Y, Sung VM, Machida K, et al. Hepatitis C virus infects T cells and affects interferon-gamma signaling in T cell lines. Virology 2007;361:161–173.
23. McDonnell TJ, Deane N, Platt FM, et al. bcl-2-immunoglobulin transgenic mice demonstrate extended B cell survival and follicular lymphoproliferation. Cell 1989;57:79–88.
24. Lacronique V, Mignon A, Fabre M, et al. Bcl-2 protects from lethal hepatic apoptosis induced by an anti-Fas antibody in mice. Nat Med 1996;2:80–86.
25. Ito T, Deng X, Carr B, et al. Bcl-2 phosphorylation required for anti-apoptosis function. J Biol Chem 1997;272:11671–11673.
26. Stern JB, Smith KA. Interleukin-2 induction of T-cell G1 progression and c-myb expression. Science 1986;233:203–206.
27. Levy Y, Brouet JC. Interleukin-10 prevents spontaneous death of germinal center B cells by induction of the bcl-2 protein. J Clin Invest 1994;93:424–428.
28. Taniguchi T, Ogasawara K, Takaoka A, et al. IRF family of transcription factors as regulators of host defense. Annu Rev Immunol 2001;19:623–655.
29. Penninger JM, Sirard C, Mittrucker HW, et al. The interferon regulatory transcription factor IRF-1 controls positive and negative selection of CD8+ thymocytes. Immunity 1997;7:243–254.
30. Lohoff M, Ferrick D, Mittrucker HW, et al. Interferon regulatory factor-1 is required for a T helper 1 immune response in vivo. Immunity 1997;6:681–689.
31. Machida K, Cheng KT, Sung VM, et al. Hepatitis C virus induces a mutator phenotype: enhanced mutations of immunoglobulin and protooncogenes. Proc Natl Acad Sci U S A 2004;101:4262–4267.
32. Machida K, Kondo Y, Huang JY, et al. Hepatitis C virus (HCV)-induced immunoglobulin hypermutation reduces the affinity and neutralizing activities of antibodies against HCV envelope protein. J Virol 2008;82:6711–6720.
33. Dolganiuc A, Paek E, Kodys K, et al. Myeloid dendritic cells of patients with chronic HCV infection induce proliferation of regulatory T lymphocytes. Gastroenterology 2008;135:2119–2127.

Received June 25, 2008. Accepted March 31, 2009.

Reprint requests

Address requests for reprints to: Michinori Kohara, PhD, Department of Microbiology and Cell Biology, Tokyo Metropolitan Institute of Medical Science, 3-18-22 Honkomagome, Bunkyo-ku, Tokyo 113-8613, Japan. e-mail: mkohara@rinshoken.or.jp; fax: (81) 3-3828-8945.

Acknowledgments

The authors thank Prof Tadatsugu Taniguchi for his scholarly support of this study; Kazuaki Inoue and Kentaro Tomita for their advice on histology; Yutaka Amako, Isao Maruyama, and Kohsuke Tanaka for technical assistance; and Mitsugu Takahashi for breeding the transgenic mice.

Conflicts of interest

The authors disclose no conflicts.

Funding

Supported in part by a research fellowship from the Japan Society for the Promotion of Science; a grant from the Ministry of Education, Culture, Sports, Science and Technology of Japan; a grant from the Ministry of Health, Labour and Welfare of Japan; and the Program for Promotion of Fundamental Studies in Health Sciences of the National Institute of Biomedical Innovation of Japan. This project was also supported by National Institutes of Health research grants P50AA11999, 5P30DK048522-13, and CA108302.

Supplementary Materials and Methods

Animal Experiments

CN2, *irf-1*$^{-/-}$, and *irf-9*$^{-/-}$ mice were maintained in conventional animal housing under specific pathogen-free conditions. AxCANCre and AxCAw1, which are replication-deficient recombinant adenoviruses that lack the E1A, E1B, and E3 regions, were obtained from Dr Izumu Saito (University of Tokyo).[1] AxCANCre expresses the Cre recombinase, whereas AxCAw1, which was used as a control, lacks the inserted *cre* gene. The Cre-expressing recombinant adenovirus (AxCANCre) and AxCAwl were expanded in HEK293 cells (kindly gifted by Dr Izumu Saito) and purified by sucrose gradient centrifugation.[1] AxCANCre or AxCAw1 (2×10^9 plaque-forming units) was injected intravenously into CN2 or nontransgenic female mice aged 9–13 weeks. The mice were killed at 4, 7, 10, 14, 21, 60, 90, 180, 400, 500, or 600 days after injection (n = 15 mice/group; total of 900 mice). Mouse behavior and phenotypes were assessed weekly, and the phenotypes were confirmed at necropsy. At necropsy, the proportion of mice with enlarged lymph nodes, according to weight, was larger in the CN2 group than in the WT group ($P < .05$). To elicit Fas-induced liver damage, adult mice were injected intravenously with 10 μg of an anti-mouse Fas monoclonal antibody that was purified from a hamster (clone Jo2; Pharmingen) in 200 μL phosphate-buffered saline (without Ca^{2+} or Mg^{2+}). Animals were observed over a 24-hour period for survival or killed at matched time points; livers were collected for histology or biochemical studies. All the animal experiments were performed according to the guidelines of the Tokyo Metropolitan Institute of Medical Science Subcommittee for Laboratory Animal Care. The protocol was approved by an institutional review board.

For CN2-29 Mx1-Cre mice, Cre expression in the liver was induced by intraperitoneal injection of poly(I:C) (GE Healthcare UK Ltd, Buckinghamshire, England). A total of 300 μL of poly(I:C) solution (1 mg/mL in phosphate-buffered saline) was injected 3 times at 48-hour intervals.

Southern Blot Analysis

Mouse livers were digested overnight at 55°C in lysis buffer (50 mmol/L Tris-HCl [pH 7.6], 100 mmol/L NaCl, 20 mmol/L EDTA, 1% sodium dodecyl sulfate) that contained 1 mg/mL proteinase K (Boehringer Mannheim, Mannheim, Germany). DNA was extracted with phenol-chloroform and precipitated with ethanol.[1] The DNA pellet was washed with 70% ethanol, dried, and resuspended in 10 mmol/L Tris (pH 7.5). Restriction endonuclease digestion with XbaI, agarose gel electrophoresis, and Southern blotting were performed using the DIG DNA Labeling and Detection System (Boehringer Mannheim). XbaI-mediated DNA fragmentation was used to examine the rate of recombination of the HCV transgene construct.[1] Recombination of the transgene (CN2) was confirmed by Southern blotting. Southern blotting of DNA samples extracted from mouse livers was performed using the DIG DNA Labeling and Detection System (Boehringer Mannheim).

Quantification of HCV Core Protein in Mouse Livers

Mouse livers were homogenized in 1 mL RIPA buffer (1% sodium dodecyl sulfate, 0.5% [vol/vol] Nonidet P40, 10 mmol/L Tris [pH 7.4], 0.15 mol/L NaCl). The HCV core protein concentrations in the liver lysates were quantified using a fluorescent enzyme immunoassay with 2 high-affinity monoclonal antibodies against the HCV core protein.[2] The HCV core protein concentration in each liver was normalized by the total protein concentration, as measured using the DC protein assay (Bio-Rad Laboratories, Hercules, CA).

Collection of Sera and Enzyme-Linked Immunosorbent Assay

To assess Fas-induced liver failure, blood samples were collected from the supraorbital veins at 0, 1, 2, 3, 4, 5, and 6 hours after administration of the Fas monoclonal antibody or by heart puncture of killed mice. Blood samples were centrifuged at 10,000*g* for 15 minutes at 4°C to isolate serum. The serum levels of IL-2, IL-4, IL-10, and IL-12 were determined using enzyme-linked immunosorbent assay kits (R&D Systems, Minneapolis, MN), according to the manufacturer's instructions. Serum alanine aminotransferase (ALT) activity was determined using a commercially available kit (Nissui, Tokyo, Japan).

Histology and Immunohistochemical Staining

Livers were frozen in Tissue-Tek OCT compound (SAKURA Finetek, Tokyo, Japan) in dry ice/ethanol, thawed, and fixed in 1:1 (vol/vol) acetone/methanol at −20°C for 10 minutes. Immunohistochemical staining was completed using tyramide signal amplification (NEN Life Science Products, Boston, MA). Nuclei were stained with 0.5 μg/mL Hoechst 33342 (Molecular Probes, Carlsbad, CA) for 1 minute at room temperature. Sections were observed under a fluorescence microscope (510 Meta; Carl Zeiss, Oberkochen, Germany). Liver samples for histology were cut into small (<1.0 cm) pieces, fixed overnight in 10% paraformaldehyde, dehydrated with ethanol, blocked in paraffin, sectioned at 10-μm thickness, stained with H&E, and viewed under a microscope (510 Meta; Carl Zeiss). For HCV core protein detection, immunohistochemistry was performed using PFA-fixed or OCT frozen sections. Tissue sections were fixed in 4% PFA and permeabilized in 0.3% H_2O_2 and methanol for 10 minutes. Antigen retrieval was achieved by autoclaving at 121°C for 5 minutes or 10 minutes or by treatment with proteinase K at 37°C for 10 minutes or 30 minutes. To detect core antigen, a mouse anti-core antibody (BT 515) and Alexa 488–conjugated streptavidin were used.

Staining was detected by the DAB substrate reaction. For CD3 and CD45R protein detection, immunohistochemistry was performed on PFA-fixed sections. Tissue sections were fixed with 4% PFA and permeabilized by treating with 0.3% H_2O_2 and methanol for 10 minutes. Antigen retrieval was achieved by autoclaving at 121°C for 10 minutes. To detect the CD3 and CD45R antigens, mouse anti-CD3 and anti-CD45R antibodies (AbD Serotec MorphoSys UK Ltd, Oxford, England) were used. Staining was detected by the addition of 3,3′-diaminobenzidine tetroxide (Dojin Kagaku, Kumamoto, Japan).

Flow Cytometry

Lymphocytes were stained with appropriate dilutions of the following antibodies: PE-conjugated anti-CD3, fluorescein isothiocyanate (FITC)-conjugated anti-B220, FITC-conjugated anti-CD4, PE-conjugated anti-CD8, FITC-conjugated anti-TCR-$\alpha\beta$, and PE-conjugated anti-TCR-$\gamma\delta$. Flow cytometry was performed using the FACSCalibur (Becton Dickinson, San Jose, CA).

Western Blot Analysis

Minced livers, lymph nodes, spleens, and splenocytes were homogenized with a Dounce glass homogenizer at 4°C in lysis buffer (1% bovine serum albumin, 1 mmol/L ethylene glycol-bis[2-aminoethylether]-*N,N,N′N′*-tetraacetic acid, 300 mmol/L sucrose, 5 mmol/L 3-[N-morpholino]propanesulfonic acid, 5 mmol/L KH_2PO_4 [pH 7.4]) that contained complete protease inhibitor cocktail (Boehringer Mannheim). After centrifugation at 27,000*g* for 15 min, 50 μg of supernatant protein were loaded in each lane of a 10% or 15% polyacrylamide gel, separated by electrophoresis in Tris-Tricine buffer (Daiichi Pure Chemicals), and transferred to polyvinylidene difluoride membranes (Amersham Life Science, Tokyo, Japan). The membranes were then incubated for 2 hours at room temperature in TBS-T (20 mmol/L Tris-HCl, 500 mmol/L NaCl, 0.1% [vol/vol] Tween 20) that contained 1% bovine serum albumin, followed by incubation with a primary antibody directed against Bcl-2 (Santa Cruz Biotechnology, Santa Cruz, CA), protein kinase R (a kind gift of Dr H. Taira, Iwate University, Japan), mouse IRF-1 (Santa Cruz Biotechnology), mouse Fas (Wako), or HCV core (31-2).[3] The membranes were washed with TBS-T, incubated with horseradish peroxidase-conjugated secondary antibodies, visualized using a chemiluminescence reagent (Amersham International, Tokyo, Japan), and detected using Hyperfilm-MP (Amersham International).

Detection of Apoptotic Cells by DNA Fragmentation

Small pieces of liver (50-80 mg in weight) were homogenized and digested overnight with proteinase K (Boehringer Mannheim) at 55°C in lysis buffer (50 mmol/L Tris-HCl [pH 7.6], 100 mmol/L NaCl, 20 mmol/L EDTA, 1% sodium dodecyl sulfate). Lysates were extracted with phenol-chloroform-isoamyl alcohol, treated with ribonuclease, precipitated with ethanol, and subjected to 2% agarose gel electrophoresis. Breaks in the hepatocyte DNA were detected using the terminal deoxynucleotidyl transferase–mediated deoxyuridine triphosphate nick-end labeling (TUNEL) assay kit (R&D Systems) according to the manufacturer's instructions.

Ribonuclease Protection Assay

The caspase transcript levels in the livers from *irf-1*$^{-/-}$ and *irf-1*$^{+/+}$ mice were determined in a ribonuclease protection assay that used mouse apoptosis multiprobe template sets (Pharmingen). Briefly, total RNA was extracted from the livers and assayed with the RiboQuant Multi-Probe RNase Protection Assay System mAPO-1 (Becton Dickinson). Multiple ^{32}P-labeled caspase probes and the control glyceraldehyde-3-phosphate dehydrogenase probe were synthesized and hybridized overnight to the target RNA, treated with ribonuclease, and separated by electrophoresis on a denaturing polyacrylamide gel. The radioactive bands representing undigested RNAs were then detected and quantified using the BAS 2000 phosphoimager (Fuji Photo Film, Tokyo, Japan). Band intensities were normalized to the glyceraldehyde-3-phosphate dehydrogenase mRNA band in the same lane.

RNA Isolation and Reverse-Transcription PCR

The mRNA species from mouse splenocytes and peripheral blood lymphocytes were isolated using Isogen (Nippon Gene, Shizouka, Japan). The core, E1, E2, NS2, and lacZ mRNA species were detected by reverse-transcription PCR using the following primers: for core-621S, 5′-gggcaggatggctcctgtca-3′; for core-831A, 5′-ttcacgccgtcctccacaac-3′; for E1-991S, 5′-agcggacatgatcatgcata-3′; for E1-1314A, 5′-atcatcatgtcccaagccat-3′; for E2-1601S, 5′-tggcacatcaacaggactgc-3′; for E2-1860A, 5′-actggaccacacaccttcga-3′; for NS2-2807S, 5′-gtgtttgtaggtctggtact-3′; for NS2-2925A, 5′-atccacacttgcaggtgcgc-3′; for lacZ 30S, 5′-aaccctggcgttacccaact-3′; and for lacZ 430A, 5′-gaaacgccgagttaacgcca-3′.

Quantitative Real-Time PCR Amplification of Cytokine and Bcl-2 mRNA Species

The RNA from 10,000 cells was used for art-PCR in the ABI Prism 7900-HT Sequence Detection System with the Universal PCR Master Mix (Applied Biosystems, Foster City, CA) and the RT2 qPCR Primer sets for murine IL-2, IL-4, IL-10, IL-12, *bcl-2,* and glyceraldehyde-3-phosphate dehydrogenase (SABioscience Inc, Frederick, MD; and Applied Biosystems), as described previously.[4] The quantitative real-time PCR results are presented as the average values from at least 3 independent experiments with duplicate PCR analyses.

Measurements of Caspase Activities Through Cleavage of Fluorogenic Substrates

The cytosolic fractions of splenocytes were isolated as described previously,[5] with some modifications. Briefly, splenocytes were homogenized in a Dounce glass homogenizer (loose type) with lysis buffer (0.3 mol/L mannitol, 5 mmol/L 3-[*N*-morpholino]propanesulfonic acid, 1 mmol/L ethylene glycol-bis[β-aminoethyl ether]-*N*,*N*,*N*′,*N*′-tetraacetic acid, 4 mmol/L KH_2PO_4, 20 μg/mL leupeptin, 10 μg/mL pepstatin A, 10 μg/mL aprotinin, 2 mmol/L phenylmethylsulfonyl fluoride) and fractionated into pellet, heavy membrane, light membrane, and cytosolic fractions. The lysates were centrifuged at 600*g* for 10 minutes at 4°C to remove debris or fibers. The supernatants were centrifuged at 10,000*g* for 15 minutes at 4°C, and the pellets were collected as the heavy membrane fractions. The supernatants were then centrifuged at 100,000*g* for 45 minutes at 4°C and collected as the cytosolic fraction. The activities of caspase-9 and caspases-3/7 were measured using Ac-LEHD-AFC or Ac-DEVD-AFC (Enzyme Systems Products, Livermore, CA) as substrates, respectively. The substrates were preincubated for 10 minutes at 37°C in reaction buffer.[6] Thereafter, 100 μg of lysate was added to 1.25 mL of the substrate reaction buffer and incubated for 60 minutes at 37°C. The fluorescence of the released 7-amino-4-trifluoromethylcoumarin was detected using a fluorescence spectrometer (μQUANT; Bio-tech Instruments, Winooski, VT), with excitation at 400 nm and emission at 505 nm. One unit of caspase activity corresponds to the activity required to cleave 1 pmol of the substrate in 60 minutes at 37°C.

Colony Formation Assay

The colony formation assay was performed by the methylcellulose membrane method, as described previously.[7,8] Briefly, splenocytes were isolated from mice, plated at 4×10^5 cells/mL in 1% methylcellulose culture medium (Methocult 3430; StemCell Technology, Vancouver, Canada) that contained 100 μL of Iscove's modified Dulbecco's medium (Invitrogen, Carlsbad, CA) with 25 μg/mL of stem cell factor (R&D Systems, Minneapolis, MN) and hemin (Sigma-Aldrich, St. Louis, MO). Cells were infected with adenovirus that expressed the cre DNA recombinase (AxCANCre) or LacZ (AxCALacZ) gene and treated with cytokines (IL-2, IL-10, IL-12, and combinations thereof). Erythroid burst-forming units, as well as granulocyte, erythrocyte, macrophage, and megakaryocyte colony-forming units, and granulocyte/macrophage colony-forming units were measured.[7,8] To purify the $CD4^+$, $CD8^+$, and $CD45R/B220^+$ cell populations, peritoneal lymph node cells were isolated using immunomagnetic beads conjugated to the corresponding antibodies (Miltenyi Biotec, Bergisch Gladbach, Germany), as described previously.[9] In our series, >95% of the purified cells expressed the indicated phenotypes, and viability was >98%.[10] Colony numbers were counted at 7, 14, and 28 days posttreatment. Colonies that contained more than 30 cells were counted under sealed codes, which obscured the identities of the samples.

Antibody Coating and Cell Stimulation

The cell stimulation experiments adhered to the published protocols.[11] The following purified monoclonal antibodies were used in the cell stimulation experiments: anti-core, anti-E1, anti-E2 (Biodesign International, Saco, MN), and anti-His6 (Qiagen, Hilden, Germany). Ninety-six–well plates were coated with the various antibodies according to published methods.[11] For the experiments involving the blocking anti-core, E1, and E2 antibodies, the recombinant proteins were first treated with the blocking antibodies at 37°C for 30 minutes. The cells were then added to the core-, E1-, E2-, or antibody-coated plates, as previously described.[12]

Statistical Analysis

Data are presented as mean ± SD. Differences were compared using the Student *t* test and considered statistically significant at $P < .05$.

Supplementary Results

Inhibition of Fas-Induced Apoptosis by Disruption of irf-1 *Leads to Persistent Expression of HCV in Transgenic Mouse Livers*

The Fas ligand is essential for the development of hepatitis via cytotoxic T-lymphocyte–mediated cell killing.[13] Therefore, we determined the sensitivity of *irf-1*$^{-/-}$ hepatocytes to Fas-induced apoptosis. The *irf-1*$^{-/-}$ mice and WT littermates were injected intravenously with an anti-Fas monoclonal antibody. All 10 *irf-1*$^{-/-}$ mice survived, whereas 4 of 10 WT littermates died within 24 hours due to acute liver failure associated with massive hepatic apoptosis and hemorrhagic necrosis ($P < .05$; Supplementary Figure 2*A*). Acute and severe liver injury was confirmed by measurement of the serum ALT levels, which were increased by up to 200-fold in WT mice within 3 hours of administration of the anti-Fas monoclonal antibody (Supplementary Figure 2*B*). In contrast, delayed and less prominent increases in serum ALT levels were observed in the *irf-1*$^{-/-}$ mice 3 hours and 6 hours after injection of the anti-Fas monoclonal antibody (Supplementary Figure 2*B*). The WT mice had severe lesions of the liver, and staining with 4′,6-diamidino-2-phenylindole revealed morphologic changes that were characteristic of apoptosis (Supplementary Figure 2*C*). Massive panlobular and multilobular apoptotic necrosis (>90%) and peliosis were observed in the *irf-1*$^{-/-}$ CN2 mice in conjunction with 20% mortality (Supplementary Figure 2*C* [*a* and *b*]). Staining using TUNEL showed significantly lower levels of Fas-induced DNA fragmentation in the *irf-1*$^{-/-}$ hepatocytes than in the WT hepatocytes

(compare Supplementary Figure 2C [*i* and *j*]), and the onset of DNA fragmentation in *irf-1*$^{-/-}$ hepatocytes was delayed compared with that in WT hepatocytes (data not shown). There were no significant injuries to other organs, such as the thymus and kidneys. Thus, the WT mice showed severe, acute Fas-induced hepatic cytolysis, whereas the *irf-1*$^{-/-}$ mice had significantly delayed serum ALT production and lower serum ALT levels, along with delayed and less severe apoptosis of liver cells, indicating that disruption of *irf-1* inhibits the Fas-induced apoptosis of hepatocytes in vivo.

Several caspases, especially caspase-7 and caspase-3, are activated to cleave cytoplasmic and cytoskeletal proteins during Fas-induced apoptosis of murine hepatocytes.[14,15] To determine the mechanism by which disruption of *irf-1* inhibits Fas-induced apoptosis of hepatocytes, we examined caspase mRNA expression in ribonuclease protection assays. The levels of caspase-1 mRNA in *irf-1*$^{-/-}$ hepatocytes were significantly lower than those in WT hepatocytes, which is in agreement with previously reported results.[16] Interestingly, the caspase-6 and caspase-7 mRNA levels were also lower in the *irf-1*$^{-/-}$ mice than in the WT mice (Supplementary Figure 2*D* and *E*). The disruption of *irf-1* did not affect the levels of Fas or protein kinase R protein (data not shown). Furthermore, the anti-Fas monoclonal antibody induced the release of comparable levels of cytochrome *c* from the mitochondria to the cytoplasm in the WT and *irf-1*$^{-/-}$ hepatocytes (data not shown). These results suggest that the reduced expression of effector caspases may delay Fas-mediated apoptosis in *irf-1*$^{-/-}$ mice and abrogate the elimination of HCV-expressing cells in vivo.

Supplementary Discussion

HCV-infected patients have elevated levels of serum IL-10 and IL-12.[17] As shown in the present study, altered cytokine production may enhance HCV-induced lymphoproliferation. IL-10-transgenic mice develop Fas ligand–mediated exocrinopathy that resembles Sjögren's syndrome.[18] This exocrinopathy was also observed in some of the HCV protein-expressing mice in the current study. Therefore, the induction of cytokine expression in HCV transgenic mice may trigger lymphomagenesis. The induction of the gene that encodes the p40 subunit of IL-12, which is essential for Th1-type differentiation of the immune system, is entirely dependent on IRF-1,[19,20] which indicates that *irf-1* disruption affects the production of IL-12. In addition, HCV core protein reportedly activates the promoter for IL-2,[21] which is a growth factor for antigen-stimulated T lymphocytes that is responsible for antigen-induced clonal expansion of T cells. The high serum concentrations of IL-2 and IL-10 may also accelerate the differentiation of memory B cells.[22] Moreover, the induction of splenocyte proliferation by treatment with IL-2 plus IL-10 was suppressed by IL-12 in *irf-1*$^{-/-}$ CN2 mice. This suggests a potential application of IL-12 therapy for lymphomas associated with HCV infection. Long-term HCV infection may result in clonal B-cell expansion of immunoglobulin-secreting lymphocytes; approximately 35% of HCV-infected patients are reported to develop B-cell lymphoma.[23] HCV infection is associated not only with non-Hodgkin's B-cell lymphoma, but also with other lymphoid and myeloid malignancies, including non-Hodgkin's T-cell lymphomas; this association is consistent with our findings, especially in the *irf-1*$^{-/-}$ HCV transgenic mouse model (Figures 3 and 6).[24–27] It is also worth clarifying whether and at what frequency polyclonal lymphoid hyperplasia precedes lymphomagenesis and whether progression from hyperplasia to lymphoma is heralded by a more striking impairment of cytokine (ie, IL-2, IL-10, or IL-12) production.

We found that Fas-induced apoptosis was significantly suppressed in *irf-1*$^{-/-}$ hepatocytes. This suppression may be related to the essential role that IRF-1 plays in the induction of caspase expression.[16,28] Almost all of the *irf-1*$^{-/-}$ CN2 mice persistently expressed higher levels of HCV core protein in the liver, as compared with the *irf-1*$^{+/+}$ CN2 mice, which suggests wither deficient immunity or inefficient induction of apoptosis in *irf-1*$^{-/-}$ lymphocytes and hepatocytes. Immune surveillance in *irf-1*$^{-/-}$ mice may not eliminate efficiently the HCV protein-expressing cells due to reductions in the numbers of natural killer[19] and CD8^{+} T cells.[9] Furthermore, IRF-1 is an essential mediator of IFN-γ–induced cell cycle arrest and apoptosis.[29] Because activated lymphocytes are normally eliminated by activation-induced cell death, we speculate that the inhibition of apoptosis of *irf-1*$^{-/-}$ lymphocytes results in the accumulation of these cells in the lymph nodes and spleen. HCV core protein also modulates the activities of IFN-induced transacting factors in the Jak/Stat signaling pathway.[30] In addition, a protein kinase R–binding domain polypeptide of the HCV NS5A protein relieves the blockade of the IRF-1 pathway, resulting in the induction of IRF-1–dependent antiviral effector genes.[31] HCV NS5A alone is sufficient to block both the activation of IRF-1 and the induction of an IRF-1–dependent cellular promoter by double-stranded RNA.[31] Therefore, blockade of the IRF-1 pathway by HCV infection may facilitate the persistent expression of HCV proteins in hepatocytes or lymphocytes, resulting in the inhibition of Fas-mediated apoptosis in *irf-1*$^{-/-}$ hepatocytes. Indeed, genetic abnormalities in the Fas pathway in humans or *lpr* mice cause an autoimmune lymphoproliferative syndrome.[32] Differential modulation of apoptosis sensitivity in CD95 type I and type II cells (hepatocytes and some T lymphocytes) has been established.[33,34] It is noteworthy that both T lymphocytes and hepatocytes have CD95 type II signaling. It is interesting that lymphomagenesis is dominant over liver tumor development. The molecular mechanism underlying this dominance remains unknown. Further molecular analysis will